Journal of Pharmaceutical Analysis 10 (2020) 130–146

Contents lists available at ScienceDirect

Journal of Pharmaceutical Analysis

journal homepage: www.elsevier.com/locate/jpa

Original article

Erucic acid from *Isatis indigotica Fort.* suppresses influenza A virus replication and inflammation *in vitro* and *in vivo* through modulation of NF-κB and p38 MAPK pathway

Xiaoli Liang [a,1], Yuan Huang [b,1], Xiping Pan [c,1], Yanbing Hao [a], Xiaowei Chen [a], Haiming Jiang [a], Jing Li [a,*], Beixian Zhou [d,**], Zifeng Yang [a,e,***]

[a] State Key Laboratory of Respiratory Diseases, Guangzhou Institute of Respiratory Health, National Clinical Centre of Respiratory Disease, The First Affiliated Hospital, Guangzhou Medical University, Guangzhou, 510120, China
[b] Hutchison Whampoa Guangzhou Baiyunshan Chinese Medicine Co., Ltd, Guangzhou, 510515, China
[c] Institute of Combination Chinese and Western Medicine, Guangzhou Medical University, Guangzhou, 511436, China
[d] Department of Pharmacy, The People's Hospital of Gaozhou, Gaozhou, 525200, Guangdong, China
[e] State Key Laboratory of Quality Research in Chinese Medicine, Macau Institute for Applied Research in Medicine and Health, Macau University of Science and Technology, Avenida Wai Long, Taipa, Macau, 999078, PR China

ARTICLE INFO

Article history:
Received 4 March 2019
Received in revised form
17 September 2019
Accepted 25 September 2019
Available online 4 October 2019

Keywords:
Influenza A virus
Isatis indigotica Fort.
Erucic acid
Antiviral
Anti-inflammatory
NF-κB
p38 MAPK
Lung injury

ABSTRACT

Isatis indigotica Fort. (Ban-Lan-Gen) is an herbal medicine prescribed for influenza treatment. However, its active components and mode of action remain mostly unknown. In the present study, erucic acid was isolated from *Isatis indigotica Fort.*, and subsequently its underlying mechanism against influenza A virus (IAV) infection was investigated in vitro and in vivo. Our results demonstrated that erucic acid exhibited broad-spectrum antiviral activity against IAV resulting from reduction of viral polymerase transcription activity. Erucic acid was found to exert inhibitory effects on IAV or viral (v) RNA-induced pro-inflammatory mediators as well as interferons (IFNs). The molecular mechanism by which erucic acid with antiviral and anti-inflammatory properties was attributed to inactivation of NF-κB and p38 MAPK signaling. Furthermore, the NF-κB and p38 MAPK inhibitory effect of erucic acid led to diminishing the transcriptional activity of interferon-stimulated gene factor 3 (ISGF-3), and thereby reducing IAV-triggered pro-inflammatory response amplification in IFN-β-sensitized cells. Additionally, IAV- or vRNA-triggered apoptosis of alveolar epithelial A549 cells was prevented by erucic acid. In vivo, erucic acid administration consistently displayed decreased lung viral load and viral antigens expression. Meanwhile, erucic acid markedly reduced $CD8^+$ cytotoxic T lymphocyte (CTL) recruitment, pro-apoptotic signaling, hyperactivity of multiple signaling pathways, and exacerbated immune inflammation in the lung, which resulted in decreased lung injury and mortality in mice with a mouse-adapted A/FM/1/47-MA(H1N1) strain infection. Our findings provided a mechanistic basis for the action of erucic acid against IAV-mediated inflammation and injury, suggesting that erucic acid may have a therapeutic potential in the treatment of influenza.

© 2019 Xi'an Jiaotong University. Production and hosting by Elsevier B.V. This is an open access article under the CC BY-NC-ND license (http://creativecommons.org/licenses/by-nc-nd/4.0/).

1. Introduction

Influenza A virus (IAV) infection is a major cause of acute respiratory tract diseases and is associated with respiratory syndromes ranging from mild to life-threatening conditions, which constitutes one of the serious threats to the public health worldwide. In 1918, the outbreak of the Spanish flu caused more than 50 million deaths [1]. In recent decades, continuing transmission of low pathogenic seasonal H1N1 or high pathogenic H5N1 and H7N9 between humans poses a pandemic threat [2–4]. Vaccination and

Peer review under responsibility of Xi'an Jiaotong University.
* Corresponding author.
** Corresponding author.
*** Corresponding author at: State Key Laboratory of Respiratory Diseases, Guangzhou Institute of Respiratory Health, National Clinical Centre of Respiratory Disease, the First Affiliated Hospital, Guangzhou Medical University, Guangzhou, Guangdong, 510120, China.
E-mail addresses: lijing82@gzhmu.edu.cn (J. Li), zbeixian@126.com (B. Zhou), Jeffyah@163.com (Z. Yang).
[1] These authors contributed equally to this work.

https://doi.org/10.1016/j.jpha.2019.09.005
2095-1779/© 2019 Xi'an Jiaotong University. Production and hosting by Elsevier B.V. This is an open access article under the CC BY-NC-ND license (http://creativecommons.org/licenses/by-nc-nd/4.0/).

antiviral drugs such as oseltamivir are efficient approaches for controlling influenza symptoms, but numerous studies reported that they are insufficiency in protecting against an emerging pandemic due to antigenic drift. Therefore, continuing efforts are required to identify novel agents that may effectively fight future influenza pandemics.

To date, the expanding understanding of the pathogenesis of influenza virus infections provided direction for the development of effective therapeutic strategies. Analysis of viral components using reverse genetics methods has elucidated their function and virulence in the pathogenicity of influenza diseases. For instance, recombinant viruses carrying PB2 segments from the 1918 pandemic H1N1 or the PB1–F2 protein are associated with enhanced inflammation and host cell death [5,6], which contribute to enhanced disease severity. Moreover, early antiviral therapy provides better therapeutic benefits but is ineffective in critically ill patients with influenza virus infection [7]. Excessive inflammation triggered by viruses is another aspect of pathogenic factors that serve a critical role in determining outcomes of viral infection. A significant correlation between the severity of clinical signs and levels of cytokines was found in humans and ferrets with seasonal influenza virus infections [8,9]. Intense pro-inflammatory responses were observed in fatal cases of high pathogenic H5N1 virus infection [10]. However, it is evident that mice deficient in cytokines or with steroid treatment were not provided a survival benefit compared with untreated mice after viral challenge [11]. A reasonable explanation for this paradox seems to be that both viral factors and the host immune response are important contributors of influenza diseases. Indeed, combination of antiviral agents with immunomodulators has been shown to effectively reduce lethal influenza virus-induced morbidity and mortality as a proof of principle [12,13].

The replication of influenza virus in host cells is dependent on a variety of intracellular signaling pathways that synchronously initiate the pro-inflammatory response to limit virus spread. Therefore, the inhibition of signaling required for viral replication exerts antiviral effects and attenuates virus-mediated excessive pro-inflammatory responses. Activation of inducible transcription factor nuclear factor-κB (NF-κB) plays essential roles in the regulation of diverse biological processes, such as immune responses to pathogen infection, differentiation, apoptosis and cell survival. In fact, NF-κB signaling plays a critical role in productive replication of influenza viruses. Cell lines with decreased NF-κB activities result in decreased susceptibility to influenza virus propagation [14]. Several studies revealed that influenza virus affects NF-κB signaling to reduce viral (v) RNA synthesis and viral ribonucleoprotein complex (vRNP) nuclear export, and thereby virus production is negatively affected by inhibitors of NF-κB [15,16]. With regard to NF-κB-mediated immune responses, inhibition of NF-κB activation or its genetic deficiency suppresses influenza virus-mediated robust production of inflammatory mediators, such as interleukin (IL)-6, IL-8, MCP-1, Rantes and IFN-β [17]. Strikingly, administration of NF-κB inhibitors protects mice against lethal influenza virus infection [18].

Additionally, activation of p38 kinase, a signaling mediator belonging to the MAPK superfamily that transduces intra- and extracellular stimuli and governs various biological processes, supports viral replication and associates with virus-associated dysregulation of inflammatory response. Previous reports revealed that p38 kinase is involved in regulating nuclear export of vRNP as well as virus entry into host cells [19,20]. In addition, results from independent studies suggested that dysregulation of pro-inflammatory cytokine expression in HPAIV-infected primary human macrophages and bronchial epithelial cells is correlated with hyperactivation of p38 kinase [21,22]. In particular, treatment with p38 kinase inhibitor (SB202190) protects mice against lethal challenges with H5N1 virus, accompanied by markedly reduced viral titers and levels of dysregulated cytokines [23]. The severity of seasonal influenza virus infection in patients is associated with p38 kinase-mediated hypercytokinemia in plasma [24]. Agents targeting the NF-κB signaling pathway and p38 kinase can limit viral replication and excessive pro-inflammatory responses, and may be promising therapeutic interventions in influenza diseases.

Isatis indigotica Fort. belongs to the plant family of Cruciferae, which is used in the treatment of colds, fever, sore throats and headaches in traditional Chinese medicine. Previous studies revealed that active components from *Isatis indigotica Fort.*, including alkaloids (e.g., cappariloside A, epigoitrin) [25,26], polysaccharides [27] and lignans (e.g., clemastanin B, lariciresinol-4-β-D-glucopyranoside) [28–30], possess anti-influenza activities, indicating that these components may be of interest in the development of drugs for influenza disease intervention. Among these active components, the monounsaturated fatty acid erucic acid has been reported to ameliorate scopolamine-induced memory impairment via activation of the PI3K-PKCζ-ERK-CREB and AKT signaling pathway [31]. However, potential beneficial properties of erucic acid against influenza have not yet been reported. In the present study, we hypothesized that erucic acid exerts a protective effect against influenza diseases and the underlying mechanism of anti-viral properties and suppression of virus-mediated pro-inflammatory responses was investigated.

2. Materials and methods

2.1. General experimental procedures

NMR spectra were recorded on a Bruker-400 spectrometer. Agilent Q-TOF 6545 mass spectrometer connected with an Agilent 1290 Infinity LC was used to acquire HRESIMS data. Analytical HPLC was applied on a Shimadzu LC-20A using a DAD-UV detector. Column chromatography utilized silica gel (200–300 mesh, Qingdao Marine Chemical Factory, Qingdao, People's Republic of China). Silica gel plates GF254 (Qingdao Marine Chemical Factory, People's Republic of China) were used for thin-layer chromatography (TLC).

Air-dried and pieces of *Isatis indigotica Fort.* (10 kg) were extracted with 95% EtOH–H_2O (3 × 100 L; 2 h each). After evaporating under reduced pressure, 1.3 kg residues were obtained. The residue was diluted with water and partitioned with CH_2Cl_2, EtOAc, and n-BuOH, successively. The EtOAc extract was concentrated in vacuum to get 260 g residues. Then the extract subjected to column chromatography on silica gel, and petroleum ether-EtOAc was used as eluent to obtain eight fractions (fractions A–H 20:1–0:1, v/v). Each fraction was detected via TLC combined with fraction B to D. Fraction B-D was applied on a CC column (silica gel) and eluted with petroleum ether-EtOAc from 20:1 to 0:1 to afford fraction 1 to 7. Fraction 3 was purified by further silica gel column chromatography to obtain a compound (25.4 mg), which was identified as erucic acid. The purity of the compound was 95% via HPLC detection.

2.2. Structural identification of erucic acid

Erucic acid was obtained as a white waxy compound. Its molecular formula, $C_{22}H_{42}O_2$, was established by the HRESIMS ion at m/z 339.3178 $[M + H]^+$ (calcd for $C_{22}H_{43}O_2$, 339.3181). ^{1}H-NMR (CD_3Cl, 400 MHz) δ: δ5.36 (2H, m, H-13,14), 2.36 (2H, J = 7.2 Hz), 2.03 (2H, m), 1.64 (2H, m), 1.28 (28H, s, CH_2), 0.89 (3H, m, $-CH_3$). ^{13}C-NMR (CD_3Cl, 100 MHz) δ: 179.89(C-1), 129.91 (C-13), 129.89 (C-14), 34.01–22.70 ($-CH_2-$), 14.13 ($-CH_3$).

2.3. Cell lines and viruses

Human embryonic kidney cells (293) and lung adenocarcinoma cells (A549) were purchased from the ATCC and maintained in Dulbecco's modified Eagle's medium (DMEM)/F12 (1:1) (Gibco; Thermo Fisher Scientific, Inc., Waltham, MA, USA) while Madin-Darby canine kidney cells (MDCK) were obtained from the ATCC and maintained in DMEM (Gibco; Thermo Fisher Scientific, Inc.,); all media were supplemented with 10% fetal bovine serum (FBS; Gibco; Thermo Fisher Scientific, Inc.,).

Influenza virus A/PR/8/34 (H1N1), A/GZ/GIRD07/09 (H1N1), A/HK/8/68 (H3N2), A/HK/Y280/97 (H9N2), A/Duck/Guangdong/1994 (H7N3) and A/FM/1/47 (H1N1) were maintained and titrated into MDCK cells.

2.4. Cytotoxicity assays

Cytotoxic effects of erucic acid on MDCK and A549 cells were determined using MTT assays. Briefly, cells were plated at 2×10^4 cells/well in 96-well plates containing 100 μL DMEM/F12 (1:1). After incubation overnight at 37 °C with 5% CO_2, cells were treated with dimethyl sulfoxide (DMSO) or two-fold serial dilutions of erucic acid (9.375 nM - 2.4 μM) for 48 h. Then, cells were washed twice with PBS and stained with MTT (0.5 mg/mL in serum free medium) for 4 h. The supernatant was removed and formazan crystals were dissolved using DMSO (100 μL). Then, plates were gently shaken for 30 min to dissolve precipitates. Absorbance at 570 nm was determined and toxicity concentration 50 (TC_{50}) values of erucic acid were calculated using the Reed-Muench method [32].

2.5. Antiviral activity assays

The antiviral activity of erucic acid against influenza viruses was evaluated in MDCK cells. Monolayers of MDCK cells were grown overnight in 96-well plates. After washing with PBS twice, cells were inoculated with 100-fold of the 50% tissue culture infectious dose ($100 \times TCID_{50}$) of the influenza virus strains including A/PR/8/34 (H1N1), A/GZ/GIRD07/09 (H1N1), A/HK/8/68 (H3N2), A/HK/Y280/97 (H9N2), A/Duck/Guangdong/1994 (H7N3) for 2 h at 37 °C. Subsequently, the viral inoculum was discarded and replaced with diluted compounds including erucic acid and the positive control oseltamivir carboxylate (TLC PharmaChem., Inc., Canada) in TPCK-trypsin (1.5 μg/mL) containing medium, followed by incubation at 37 °C for 48 h. The cytopathic effect (CPE) was visualized under a light microscope (DM 3000; Leica Microsystems GmbH, Wetzlar, Germany). The 50% inhibitory concentration (IC_{50}) for influenza virus inhibition by the compounds was determined using the Reed-Muench method [32] and the selectivity index (SI) was defined as the ratio of TC_{50} to IC_{50}.

MDCK cells in 6-well plates were infected with influenza viruses (100 PFU/well) and incubated with the indicated concentration of compounds or DMSO. The culture supernatant containing viral particles was collected at 24 h post infection (p.i.) and stored at −80 °C. Then, MDCK cells were infected with 10-fold serial dilutions of the supernatant. Cells were stained with trypan blue after 48 h to visualize virus plaques.

For the plaque assay, confluent monolayers of MDCK cells (6×10^5 cells/well) grown in 6-well plates were inoculated with 100 PFU/well indicated influenza virus diluted in serum-free DMEM and incubated at 37 °C for 2 h to allow initiation of infection. Then, cells were washed twice with PBS to remove unbound virus and covered with DMEM containing 0.8% agarose in the presence or absence of the compounds. Plates were inverted and incubated at 37 °C for 3 days. Cells were fixed using 10% formaldehyde and stained with 0.1% crystal violet for visualization of the viral plaques.

2.6. Animal experiments

All animal experiments were approved by the Guangzhou Medical University Ethics Committee of Animal Experiments and performed in strict accordance with the Guide for the Care and Use of Laboratory Animals of the National Institutes of Health. Female BALB/c mice (age, 4–6 weeks; weight, 18–20 g) were obtained from Guangdong Medical Laboratory Animal Center and housed under specific pathogen-free conditions at the Guangzhou State Key Laboratory of Respiratory Diseases. Mice were randomly divided into five groups: Control group (non-infected); influenza virus-infected group; erucic acid high dose treatment groups, erucic acid low dose treatment groups, intragastric administration of erucic acid (50 or 100 mg/kg/day for 7 days) at 2 days prior to viral infection; oseltamivir phosphate treatment group, intragastric administration of oseltamivir phosphate (60 mg/kg/d, for 7 days) at 2 days prior to viral challenge. For viral infection, mice were anesthetized by inhalation of 5% isoflurane and inoculated intranasally with 5 LD_{50} of mouse-adapted A/FM/1/47(H1N1) influenza virus.

2.7. Lung histopathology and immunohistochemical staining

At day 5 p.i., mice were sacrificed and lung tissues were harvested. Paraformaldehyde-fixed paraffinized lung sections (4-μm) were deparaffinized and dehydrated. Lung sections were stained with hematoxylin and eosin for histopathology analysis. For immumohistochemistry, lung sections were microwaved for 20 min in 10 mM citrate buffer (pH 6.0) for antigen retrieval. Hydrogen peroxide (H_2O_2; 3%) was used to block peroxidase activity. Sections were blocked with 5% BSA in TBST for 1 h at room temperature and incubated with rabbit anti-mouse CD3 antibody in the humidified chamber for overnight at 4 °C, followed by incubation with horseradish peroxidase (HRP)-conjugated secondary antibody (1:200; Multi-Sciences). Sections were developed with DAB reagent (Maixin, China) and counterstained with hematoxylin.

2.8. Antibodies and Western blotting

Primary antibodies against P65, phosphorylated (P)–P65, P38, P–P38, ERK1/2, P-ERK1/2, JNK, P-JNK, AKT, P-AKT, STAT1, P-STAT1^{Y701}, STAT3, P-STAT3^{Y705}, COX-2, granzyme B and GAPDH were purchased from Cell Signaling Technology. Antibodies against pro-caspase3, PARP and caspase-3 (active form) were from Gentex. The antibody against CD3 was obtained from Abcam. Horseradish peroxidase (HRP)-labeled secondary antibodies were from Multi-Sciences. Human recombinant TNF-α and IFN-β were from PeproTech.

Total protein extracts from lung tissues or cells were prepared in ice-cold radioimmunoprecipitation assay (RIPA) lysis buffer (Thermo) supplemented with protease and phosphatase inhibitors (Sigma). After incubation on ice for 30 min, crude protein extracts were clarified by centrifugation at 10,000 × g for 15 min at 4 °C and aliquots of the supernatant were stored at −80 °C. Protein concentrations were determined with a BCA protein assay kit (Thermo) and equal amounts of protein were resolved on 10% SDS polyacrylamide gels. Then, proteins were transferred to PVDF membranes and immunoblotted with indicated antibodies. After incubation with HRP-labeled secondary antibody, signals were developed using an ECL detection system (PerkinElmer). The relative intensities of the protein bands were determined using ImageJ 1.44P.

2.9. Flow cytometry analysis

For apoptosis analysis, adherent cells were detached by trypsinization and suspended in 500 μL 1 × binding buffer. Then, cells were incubated with 5 μL Annexin V-FITC and 5 μL propidium iodide (PI) in the dark for 30 min at room temperature. Within 4 h, the percentage of early and late apoptotic cells was determined by the NovoCyte flow cytometer.

Bronchoalveolar lavage fluid (BALF) from mice was obtained by washing the lungs with 0.6 mL PBS three times. After centrifugation (500 × g; 5 min), BALF supernatants were collected and stored at −80 °C. BALF cell suspensions (1×10^6 cells/100 μL) were collected and stained with FACS buffer (2% BSA with 0.01% azide in PBS). Cells were then stained with fluorescein-labeled anti-mouse mAbs purchased from eBioscience for 30 min at 4 °C: CD45-APC-eFluor780 (clone NO.30-F11), CD3-PE-Cyanine7 (clone NO. UCHT1), CD4-FITC (clone NO. RM4-5) and CD8-APC (clone NO. 53–6.7). After staining, cells were washed twice and resuspended in 300 μL FACS buffer for analysis on a NovoCyte flow cytometer.

2.10. Luminex assay

Secretion levels of pro-inflammatory mediators in the culture medium and BALF were determined by Luminex assay according to the manufactures′ instructions. Multiplex assay kits for determination of human cytokines in the culture medium were purchased from Bio-Rad. Multiplex assay kits for interferons (IFN-β and IFN-λ1) and mouse cytokine detection were purchased from eBioscience.

2.11. 5′ppp RNA generation and transfection procedures

Influenza virus-infected A549 cells derived vRNA (5′ppp-RNA) was prepared using the TRIzol reagent (Invitrogen). The 5′-terminal triphosphate was removed using calf intestine alkaline phosphatase (CIAP; Takara) following the manufacturer's protocol. As a negative control, cellular RNA was obtained from uninfected cells. Cells were transfected with 500 ng/mL vRNA or cellular RNA using Lipofectamine 2000 (Invitrogen) in 6-well plates for 24 h.

2.12. Transient transfection and luciferase assay

The effect of erucic acid on viral minigenome reporter systems was assessed as described previously [33]. Briefly, components of the vRNP complex, including PB1, PB2, PA and NP, together with a luciferase reporter plasmid PHY-luci and phRL-TK plasmid were co-transfected into A549 cells. At 6 h post-transfection, cells were treated with or without erucic acid for 24 h and lysed to determine luciferase activity using the dual-luciferase reporter assay system (Promega).

Transfection of the ISRE luciferase reporter plasmid into A549 was performed as previously described. Briefly, cells grown in 96-well plates were co-transfected with 100 ng pISRE-TA-luc (Beyotime) and 10 ng pRL-TK control plasmids (Promega) by using Lipofectamine 2000 (Invitrogen) for 6 h. Subsequently, transfected cells were stimulated with influenza virus (MOI = 0.1) or IFN-β (500 ng/mL) in the presence or absence of erucic acid for 24 h.

For NF-κB activity assays, 293 cells stably expressing pNF-κB-TATA-F-Luc and pQCXIP-eGFP were infected with influenza virus (MOI = 0.1) in the presence or absence of erucic acid for 24 h. Cells were lysed for luciferase activity measurements using the luciferase assay kit (Promega). Results are presented as ratio of firefly luciferase activities normalized to *Renilla* luciferase activities or to EGFP fluorescence intensity.

2.13. Data analysis

Results are presented as the mean ± standard error of the mean (SEM). Statistical analyses were performed using SPSS 18.0 and one-way ANOVA analysis of variance followed by Newman-Student-Keuls tests were performed. Survival was analyzed using Kaplan-Meier. $P < 0.05$ was considered to indicate a statistically significant difference.

3. Results

3.1. Structure analysis of erucic acid and its cellular cytotoxicity

The chemical structure of the compound isolated from *Isatis indigotica Fort.* was elucidated by NMR spectroscopy. White amorphous powder, ^{1}H NMR (400 MHz, $CDCl_3$): δ = 5.36 (2H, m, H-13,14), 2.36 (2H, t, J = 7.3 Hz, H-2), 2.02 (4H, m, H-2,15), 1.63 (2H, m, H-3), 1.5–1.1 (28H, m, 14×CH_2), 0.90 (3H, t, J = 6.0 Hz, H-22). ^{13}C NMR (100 MHz, $CDCl_3$): δ = 179.89 (C-1), 34.01 (C-2), 24.68 (C-3), 27.21 (C-4), 129.89 (C-13), 129.91 (C-14), 29.0–32.0 (14×CH_2), 22.70 (C-21), 14.13 (C-22). The compound was identified as erucic acid by comparison with literature ^{1}H and ^{13}C-NMR spectra (Fig. 1A and B). Erucic acid induces biological effects at certain concentrations; therefore, we performed MTT assays to evaluate cytotoxic effects of erucic acid on A549 cells (Fig. 1C). The results showed that the TC_{50} value of erucic acid was 1.78 mM. Then 0.9 mM erucic acid was selected as the maximum dose for investigating the mechanism of action against virus infection.

3.2. Anti-influenza effects of erucic acid in vitro

The CPE assay was performed to study the efficacy of erucic acid against influenza A viruses. Our results showed that erucic acid treatment significantly reduced the CPE in MDCK cells induced by five influenza virus strains, including A/PR/8/34 (H1N1), A/GZ/GIRD07/09 (H1N1), A/HK/8/68 (H3N2), A/HK/Y280/97 (H9N2) and A/Duck/Guangdong/1994 (H7N3), with IC_{50} values ranging between 0.49 and 1.24 mM and SI values of 1.44–3.65 (Table 1). As shown in Figs. 2A and B, antiviral effects of erucic acid were further confirmed by plaque reduction assay (PRA) and progeny virus reduction assay. Next, we employed hemagglutinin (HA) and neuraminidase (NA) inhibition assays to test whether the antiviral property of erucic acid was attributed to its inhibitory effect on viral HA and NA. Interestingly, the data suggested that erucic acid did not interfere with viral HA and NA activities (data not shown). Furthermore, we employed IAV minigenome assays for determining the transcription activity driven by the viral polymerase in the presence of erucic acid. Erucic acid treatment exhibited significant decreases in luciferase activity in a dose-dependent manner (Fig. 2C). These results indicated that erucic acid exerted anti-influenza virus efficacy via inhibition of viral polymerase transcription activity.

3.3. Erucic acid inhibits IAV-induced NF-κB and p38 MAPK activation

Cell signaling manipulated by viruses can support viral replication [34]. To further elucidate the underlying mechanisms regarding the antiviral action of erucic acid, Western blot analysis of targets of cellular signaling was performed. Representative Western blot images in Fig. 3A suggested that MAPK (P38, ERK1/2 and JNK), NF-κB and AKT signaling pathways were activated by influenza A virus infection. Moreover, we observed that the activation of p38 MAPK and NF-κB signaling pathways was inhibited by erucic acid in a dose-dependent manner; however, the ERK1/2 MAPK, JNK

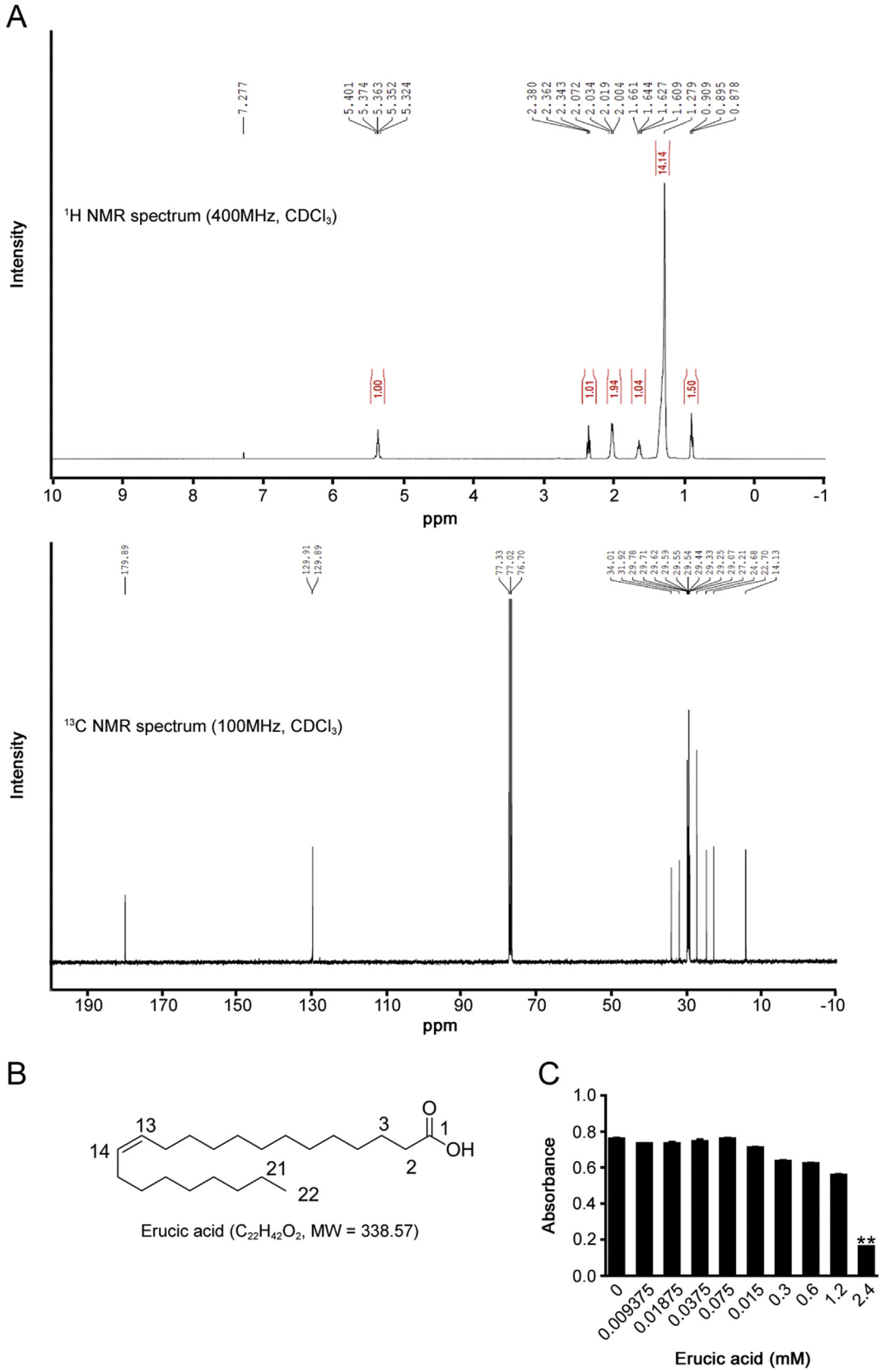

Fig. 1. Chemical structure and cytotoxicity of erucic acid. (A) ^{1}H and ^{13}C-NMR spectra for the compound isolated from *Isatis indigotica Fort.* recorded in CDCl$_3$. (B) Chemical structure of erucic acid. (C) Cytotoxic effects of erucic acid on viability of A549 cells. A549 cells were incubated with varying concentrations of erucic acid for 48 h and viability was determined by MTT assay. Data are presented as the mean ± standard error of the mean, representative of three independent experiments. *P < 0.01 vs. untreated control.

MAPK and AKT signaling pathways were not affected. Next, the effect of erucic acid on virus-induced transcriptional activities in 293 cells which were stably transfected with NF-κB-luc was investigated. Consistent with the Western blot data, erucic acid treatment resulted in decreased virus-induced NF-κB transcriptional activity (Fig. 3B). Given that the reduction of the viral polymerase transcription activity was caused by erucic acid, it became necessary to clarify whether the inhibitory effect on viral polymerase transcription activity was associated with p38 MAPK and NF-κB inhibition. As expected, the combination of p38 MAPK and NF-κB inhibitors and erucic acid caused an additive effect on the inhibition of viral polymerase transcription activity (Fig. 3C). The above results indicated that erucic acid treatment inhibited virus-induced activation of p38 MAPK and NF-κB signaling, which may be associated with anti-influenza virus efficacy.

3.4. Erucic acid inhibits IAV-triggered pro-inflammatory mediator production

Increased production of cytokines mediated by aberrant signaling contributes to the severity and mortality of influenza diseases [35]. Since erucic acid suppressed activation of p38 MAPK and NF-κB signaling, it was investigated whether erucic acid would affect virus-induced cytokines and chemokines excessive release by using Luminex assays. The cytokine profile revealed that infection with influenza A virus resulted in a significant elevation of an array of cytokines and chemokines, including IL-6, TNF-α, IP-10, RANTES, IFN-γ, IL-1β, IL-17A, IL-17F, IL-21, IL-25, IL-31 and sCD40L (Fig. 4A). Treatment with erucic acid was found to significantly decrease expression levels of these cytokines and chemokines in a dose-dependent manner (Fig. 4A). Additionally, it has been revealed that expression levels of COX-2, induced by p38 MAPK and NF-κB signaling [36,37], were associated with the pathogenesis of influenza infection. Therefore, we suggested that erucic acid may decrease virus-induced expression of COX-2. As expected, treatment of virus-infected cells with erucic acid inhibited COX-2 and derived prostaglandin E2 (PGE2) expression (Figs. 4B and C). These results demonstrated that erucic acid treatment impaired virus-induced production of pro-inflammatory mediators through inhibition of the p38 MAPK and NF-κB signaling pathways.

3.5. Erucic acid inhibits pro-inflammatory response and apoptosis in cells with IAV-derived vRNA stimulation

Apart from lung injury caused by an imbalanced overproduction of pro-inflammatory mediators, lung damage is worsened by apoptosis induction during influenza virus infection [38]. In this regard, the effect of erucic acid on influenza virus-induced apoptosis in A549 cells was determined. Annexin V staining revealed that erucic acid significantly decreased the percentages of apoptotic cells (Fig. 5A). Additionally, treatment with erucic acid exerted significant anti-apoptotic effects as determined by Western blot analysis of expression of cleaved caspase-3 and PARP in influenza virus-infected cells (Fig. 5B). It is well established that viral products such as vRNA, containing a 5′ppp end groups, NS1, PB1–F2 and M2 serve a crucial role in inducing apoptosis [5,39–41]. Therefore, effects of erucic acid on apoptosis in cells transfected with vRNA derived from IAV were analyzed. Supporting data were obtained, describing the induction of apoptotic cells and expression levels of cleaved caspase-3 and PARP after transfection with vRNA and effects were reversed by erucic acid treatment (Figs. 5C and D). Based on previous results that showed erucic acid treatment blocked IAV-induced p38 MAPK and NF-κB signaling activation (Fig. 3A), we therefore questioned whether the transfected vRNA-mediated signaling was affected by erucic acid treatment. NF-κB and p38 MAPK signaling was activated by vRNA transfection following inhibition by erucic acid treatment; however, ERK MAPK signaling was not affected (Fig. 5E). Additionally, cells transfected with vRNA triggered upregulation of the pro-inflammatory cytokines, including IL-6, TNF-α, IP-10, IL-8, MCP-1, MCP-2 and RANTES that were decreased by erucic acid treatment (Fig. 5F). Additionally, increased expression of COX-2 and its downstream product PGE2 in the culture supernatant by vRNA stimulation were abrogated by erucic acid treatment in a dose-dependent manner (Figs. 5G and H). Of note, cellular (c) RNA or the 5′ppp of vRNA removed by treatment with CIAP did not induce apoptosis, signaling transduction and pro-inflammatory mediator production. The data suggested that erucic acid inhibited pro-inflammatory responses and apoptosis in cells with vRNA stimulation through inhibition of NF-κB and p38 MAPK signaling, which might significantly attenuate IAV-induced lung injury.

3.6. Erucic acid decreases pro-inflammatory response in IAV-infected cells with IFN pre-treatment

IFNs released by host cells are vital cytokines in response to viral infection. Previous reports have shown that NF-κB and p38 MAPK signaling cascades are essential for initiation of IFNs expression [42,43]. To investigate whether erucic acid affects virus-induced expression of IFNs by targeting NF-κB and p38 MAPK signaling, IFNs levels were quantified in culture supernatants after erucic acid treatment. As shown in Fig. 6A, in virus-infected cells with erucic acid treatment, NF-κB inhibitor BAY11-7082 (column 8) and p38 MAPK inhibitor SB203580 (column 6) treatment resulted in suppression of type I INF (IFN-β) and III INF (IFN-λ1) production. Combined treatment with the two inhibitors generated synergistic effects (Fig. 6A, column 10), suggesting NF-κB and p38 MAPK signaling were critical for maximum IFNs expression. Furthermore, we observed that the combination of erucic acid with an inhibitor enhanced the inhibitory effects on the expression of IFNs (Fig. 6A, column 7 and 9). This indicated that IFN suppression effects by erucic acid were potentially associated with NF-κB and p38 MAPK

Table 1
Antiviral activity of erucic acid against influenza viruses.

Virus strain	Erucic acid			Oseltamivir		
	TC_{50} (mM)[a]	IC_{50} (mM)[b]	SI[c]	TC_{50} (μM)[a]	IC_{50} (μM)[b]	SI[c]
A/PR/8/34 (H1N1)	1.80 ± 0.06	0.55 ± 0.08	3.30 ± 0.47	>2500	1.22 ± 0.08	>1000
A/GZ/GIRD07/09 (H1N1)	1.80 ± 0.06	0.50 ± 0.08	3.61 ± 0.52	>2500	1.76 ± 0.03	>1000
A/HK/8/68 (H3N2)	1.80 ± 0.06	1.04 ± 0.11	1.74 ± 0.15	>2500	8.31 ± 0.03	>200
A/HK/Y280/97 (H9N2)	1.80 ± 0.06	0.49 ± 0.09	3.65 ± 0.62	>2500	9.93 ± 0.34	>200
A/Duck/Guangdong/1994 (H7N3)	1.80 ± 0.06	1.24 ± 0.15	1.44 ± 0.25	>2500	24.18 ± 1.53	>100

[a] TC_{50} was determined using an MTT assay.
[b] IC_{50} was determined by plaque reduction assay.
[c] The selectivity index (SI) was determined as the TC_{50}/IC_{50} ratio.

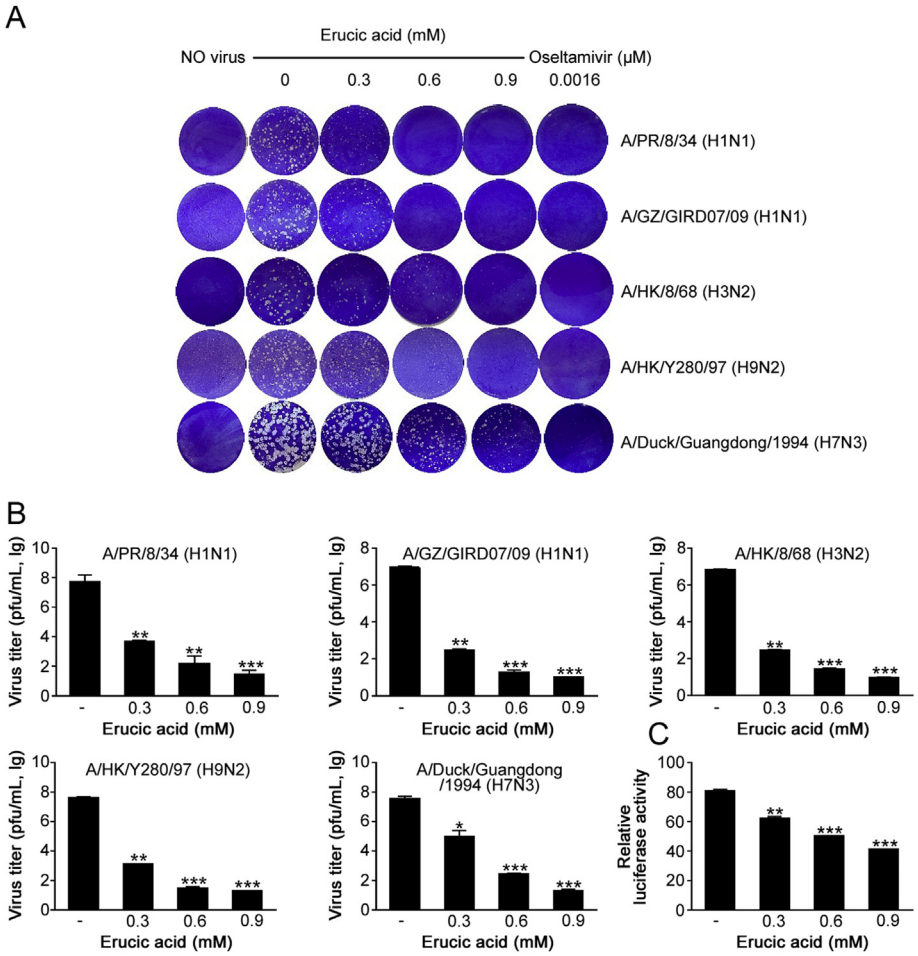

Fig. 2. Antiviral effect of erucic acid in vitro. (A) Erucic acid inhibited IAV-induced plaque formation in MDCK cells. Monolayers of MDCK were inoculated with influenza virus (A/PR/8/34 [H1N1], A/GZ/GIRD07/09 [H1N1], A/HK/8/68 [H3N2], A/HK/Y280/97 [H9N2] and A/Duck/Guangdong/1994 [H7N3]; 100 PFU/well) for 2 h, prior to treatment with different concentrations of erucic acid for 48 h. Plaque reduction assays were performed. (B) Erucic acid inhibited the production of progeny viruses. MDCK cells were infected with influenza virus (A/PR/8/34 [H1N1], A/GZ/GIRD07/09 [H1N1], A/HK/8/68 [H3N2], A/HK/Y280/97 [H9N2] and A/Duck/Guangdong/1994 [H7N3]; MOI = 0.1) and incubated for 24 h in the presence or absence of erucic acid. Culture supernatants were collected and progeny virus titers were determined. Data are presented as the mean ± standard error of the mean, representative of three independent experiments. *$P < 0.05$, **$P < 0.01$ and ***$P < 0.001$ vs. non-treated group. (C) Erucic acid reduced viral polymerase activity. IAV minigenome reporter assays were performed. Data are presented as the mean ± standard error of the mean, representative of three independent experiments. **$P < 0.01$ and ***$P < 0.001$ vs. untreated cells.

signaling inhibition properties. Erucic acid suppressed increases of IFN levels induced by vRNA (Fig. 6B). It has been reported that the immunomodulatory properties of IFNs contribute to deleterious outcomes of viral infection [44]. To investigate effects of erucic acid on IFN-associated inflammatory responses, cells were pre-treated with IFN-β (500 ng/mL) for 4 h prior to IAV infection in the presence and absence of erucic acid. Pretreatment with IFN-β significantly amplified expression of pro-inflammatory cytokines, including IL-6, IP-10, IL-8 and MIP-1β (Fig. 6C). Whereas, the pro-inflammatory amplification effect elicited by IFN-β was diminished by either erucic acid or two inhibitors (BAY11-7082 and SB203580) treatment. Of note, combination of erucic acid and the two inhibitors caused an additive effect on inhibition of cytokine expression (Fig. 6C).

To further assess the mechanisms by which erucic acid abrogated IFN-mediated pro-inflammatory responses, reporter gene assays to analyze IFN-β signaling in cells with transient ISRE reporter plasmid transfection were performed. It was observed that IAV-induced ISRE transcriptional activities were inhibited by single treatment with erucic acid or NF-κB and p38 kinase inhibitors and combination treatment led to a further reduction (Fig. 6D). Furthermore, experiments were conducted to investigate the ISRE transcriptional activities in ISRE reporter plasmid transfected-cells stimulated with IFN-β prior to IAV infection. It was observed that the ISRE transcriptional activity was significantly higher in IAV-infected cells pretreated with IFN compared with untreated cells. Transcriptional activity was partially reduced by erucic acid and NF-κB or p38 kinase inhibitor treatment, and in combination, treatment led to a further reduction (Fig. 6E). Collectively, these data suggested that the transcriptional activity of ISRE was suppressed by erucic acid treatment, thus dampening the amplification of pro-inflammatory responses in cells pre-treated with IFN-β via the inhibition of NF-κB and p38 MAPK signaling.

3.7. Erucic acid protects mice from IAV-induced lung injury and mortality

To further evaluate pharmacological effects of erucic acid in vivo, mice were intragastrically administered with ration of erucic acid at two days prior to challenge with 5 LD_{50} of mouse-adapted H1N1 influenza strain (A/FM/1/47). On day 7 p.i., IAV-infected mice exhibited pronounced clinical symptoms, including

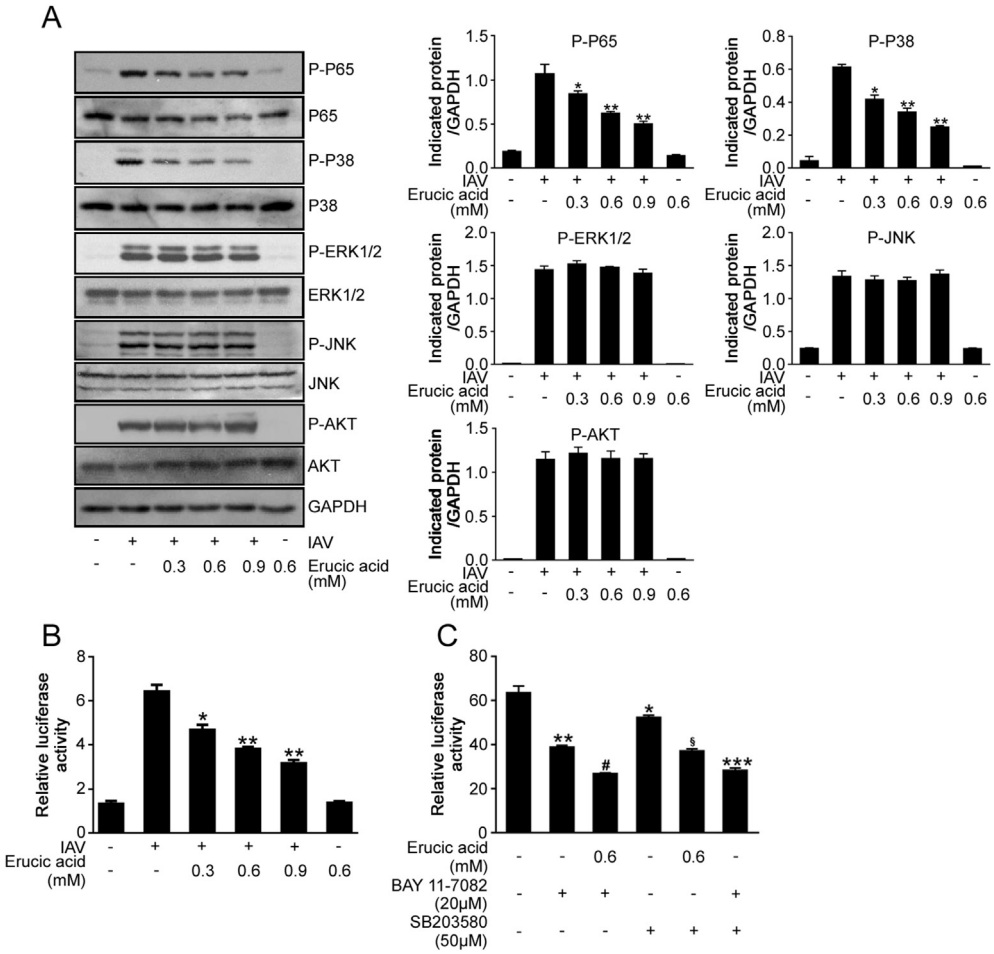

Fig. 3. Erucic acid inhibits NF-κB and p38 MAPK signaling after IAV infection. (A) A549 cells were infected with A/PR8/34(H1N1) (MOI = 0.1) and incubated with or without erucic acid for 24 h prior to Western blot analysis. Phosphorylated and total NF-κB (p65), MAPKs and AKT were detected with specific antibodies; GAPDH served as loading control. Data are presented as the mean ± standard error of the mean, representative of three independent experiments. $^{*}P < 0.05$, $^{**}P < 0.01$ vs. IAV-infected. (B) Analysis of NF-κB transcription activity. NF-κB-luc reporter plasmid was transfected into 293 cells and cells were inoculated with A/PR8/34(H1N1) (MOI = 0.1) for 2 h prior to 24 h treatment with different concentrations of erucic acid. Cells were assayed for luciferase activity. Data are presented as the mean ± standard error of the mean, representative of three independent experiments. $^{*}P < 0.05$, $^{**}P < 0.01$ vs. IAV-infected. (C) Combination of p38 MAPK and NF-κB inhibitors, and erucic acid treatment reduced viral polymerase activity. IAV minigenome-based reporter system-transfected cells were treated with or without p38 MAPK of NF-κB inhibitors. For the combined treatment cells were incubated with erucic acid for further 24 h and assessed using the dual-luciferase reporter assay system. Data are presented as the mean ± standard error of the mean, representative of three independent experiments. $^{*}P < 0.05$, $^{**}P < 0.01$ and $^{***}P < 0.001$ vs. untreated cells; $^{\#}P < 0.05$ vs. BAY11-7082-treated (column 2); $^{\S}P < 0.05$ vs. SB203580-treated (column 4).

piloerection, reduced physical activity, hunched posture, swaying gait and labored breathing, and erucic acid-administered mice exhibited relieved disease symptoms or none (Fig. 7A). Similar results were observed when monitoring the survival rate and body weight loss of virus-infected mice. As shown in Fig. 7B, virus-infected mice with 50 or 100 mg/kg/day erucic acid treatment revealed increased survival rates compared with untreated mice (80% and 100%, respectively, vs. 0%). In addition, continuous weight loss caused by viral infection was reversed by erucic acid treatment (Fig. 7C). Differences in morbidity were reflected in lung injury, where pretreatment with 50 or 100 mg/kg/day erucic acid significantly decreased the lung index and protein concentrations in the BALF (Figs. 7D and E). Furthermore, it was observed that erucic acid decreased virus titers and expression of virus antigens, including PB1, PB2 and M1 in the lung (Figs. 7F and G). Furthermore, histopathological examination of lung tissues revealed viral infection triggered massive inflammatory cell infiltration leading to extensive alveolar airspace destruction, which was significantly ameliorated by erucic acid treatment (Fig. 7H, upper panel). In addition, immunohistochemical analysis suggested that $CD3^{+}$ immunocytes were enriched in mice infected with IAV compared with mice receiving erucic acid treatment (Fig. 7H, lower panel). In line with this, virus-mediated $CD3^{+}CD8^{+}$ cytotoxic T lymphocyte (CTL) recruitment in BALF was significantly reduced by erucic acid treatment (Fig. 7I). Although antigen-specific $CD3^{+}CD8^{+}$ T cells are essential for pathogen elimination, inappropriate cytolytic activity mediated by CTL-released pro-apoptotic enzyme granzyme B contributes to lung injury. Erucic acid reduced the levels of granzyme B and active caspase-3 in lung homogenates (Fig. 7J). Together, these results suggested that erucic acid protected mice from IAV-mediated lung injury and mortality, which was correlated with its anti-viral properties and thereby reduction of CTL recruitment.

3.8. Erucic acid decreases IAV-induced excessive pro-inflammatory response by interfering with multiple signaling pathways

To provide insights into the mechanism of action of erucic acid in IAV infection in vivo, effects of erucic acid on IAV-mediated signal transduction and pro-inflammatory responses in the lung were

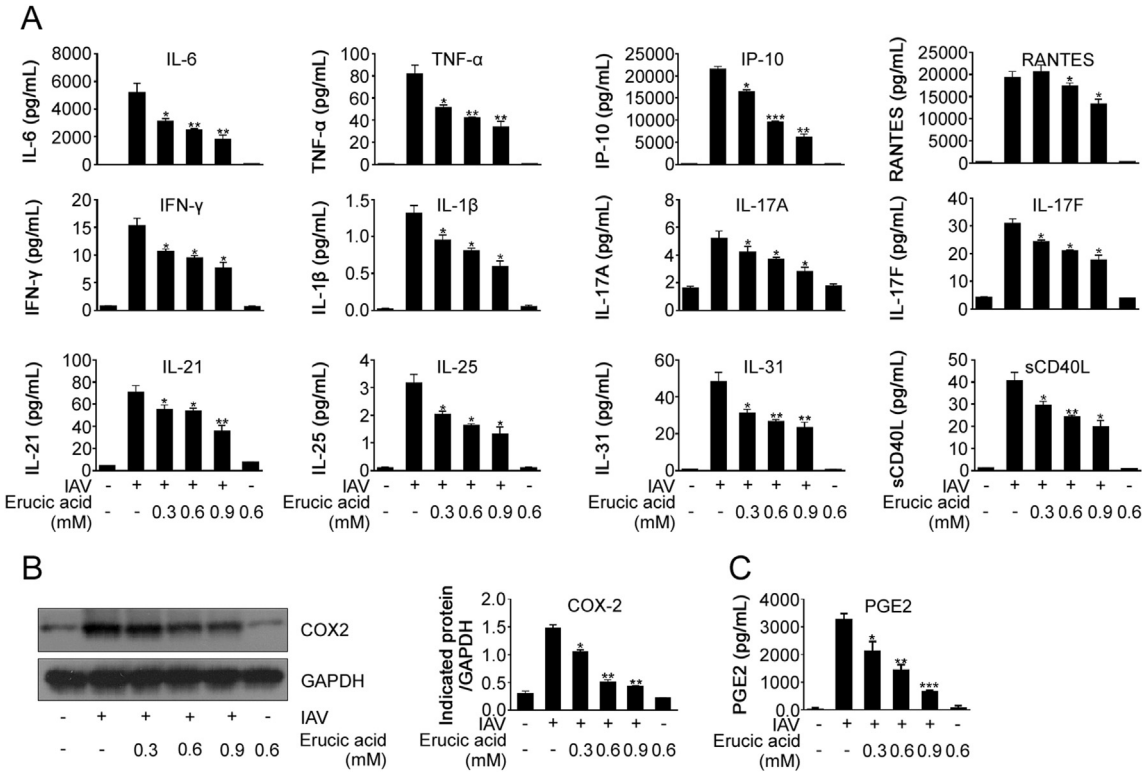

Fig. 4. Erucic acid reduces IAV-induced expression of pro-inflammatory mediators. (A) Levels of cytokines and chemokines were determined by Luminex assays in the culture supernatant of A549 cells that were infected with A/PR8/34(H1N1) (MOI = 0.1) and treated with or without erucic acid. (B–C) A/PR8/34(H1N1)-infected A549 cells were incubated with erucic acid for 24 h; total proteins or culture supernatant were collected for analysis of COX-2 and PGE2 levels by Western blot or ELISA, respectively. Data are presented as the mean ± standard error of the mean, representative of three independent experiments. *$P < 0.05$, **$P < 0.01$ and ***$P < 0.001$ vs. IAV-infected.

assessed. It was found that erucic acid significantly decreased IAV-mediated phosphorylation levels of p38 MAPK, ERK MAPK, STAT1, STAT3 and AKT signaling in the lung (Fig. 8A). These results suggested that inhibition of these signaling pathways via erucic acid may attenuate IAV-mediated excessive expression of pro-inflammatory cytokines, which contributes to severe lung immunopathology. Additionally, it was demonstrated that erucic acid administration inhibited levels of pro-inflammatory cytokines in the BALF, including IL-6, TNF-α, MCP-1, MIP-1α and GM-CSF, and lung tissue, including IL-6, IP-10, MCP-1 and RANTES (Figs. 8B and C). As results from the in vitro analysis suggested that erucic acid reversed IAV-induced expression of IFNs associated with amplification of pro-inflammatory response, it was important to determine whether erucic acid affected the levels of IFNs in vivo. As expected, members of type I IFNs (IFN-α/β) were reduced by erucic acid treatment (Fig. 8D). Furthermore, it was found that the anti-inflammatory cytokine IL-10, terminating inflammation, was elevated by erucic acid treatment (Fig. 8E). The data provided insights into the pharmacological mechanisms of erucic acid that attenuated dysregulated pro-inflammatory responses through inhibition of aberrant signaling cascades linked to influenza severity.

4. Discussion

Seasonal epidemics and occasional pandemics of influenza viruses constitute a serious public health risk and inflict immense morbidity and mortality. Antiviral drugs are used clinically in influenza therapy; however, even early oseltamivir treatment does not improve the outcome of critically ill patients with HPAI H5N1 or H7N9 virus infection due to induction of an uncontrollable cytokine storm [10,45]. Clinical evidence demonstrated an association of influenza pathogenesis with the intensity of the inflammatory response, highlighting the potential benefits of immunomodulatory agents for influenza treatments. Nevertheless, given that viral PAMPs are detected by cellular PRRs and subsequently evoke pro-inflammatory responses, the development of dual-functional drugs with both antiviral and anti-inflammatory properties shows potential in the treatment of hypercytokinemia in severe influenza cases. Antiviral activity further acts to reduce inflammation by decreasing the presence of PAMPs to be sensed by cellular PRRs.

Viral load is a critical contributor in the pathogenesis of influenza diseases. Erucic acid presented efficiency against several strains of human influenza viruses, including A/PR/8/34 (H1N1), A/GZ/GIRD07/09 (H1N1), A/HK/8/68 (H3N2), A/HK/Y280/97 (H9N2) and A/Duck/Guangdong/1994 (H7N3) (Table 1). Its antiviral properties were confirmed by plaque reduction and progeny virus yield reduction assays (Figs. 2A and B). In addition, virus titers and viral antigens were decreased in mice treated with erucic acid (Figs. 7F and G). In vitro and in vivo experiments demonstrated that inhibition of NF-κB and p38 kinase signaling pathways inhibited viral replication [16,23]. Treatment with specific NF-κB or p38 kinase inhibitors blocked nuclear-cytoplasmic translocation of viral ribonucleoproteins and thereby reduced virus titers [16,20]. Inhibition of the NF-κB signaling pathway effectively impairs transcriptional activities of the viral polymerase complex [15]. In this study, data revealed that erucic acid treatment suppressed the influenza virus-mediated activation of NF-κB and p38 MAPK signaling in vitro and in vivo (Figs. 3A and B and 8A). Additionally, viral polymerase transcription activity was reduced further by co-treatment with erucic acid and NF-κB or p38 MAPK inhibitors (Fig. 3C). Therefore, it was proposed that inhibition of influenza virus-mediated activation

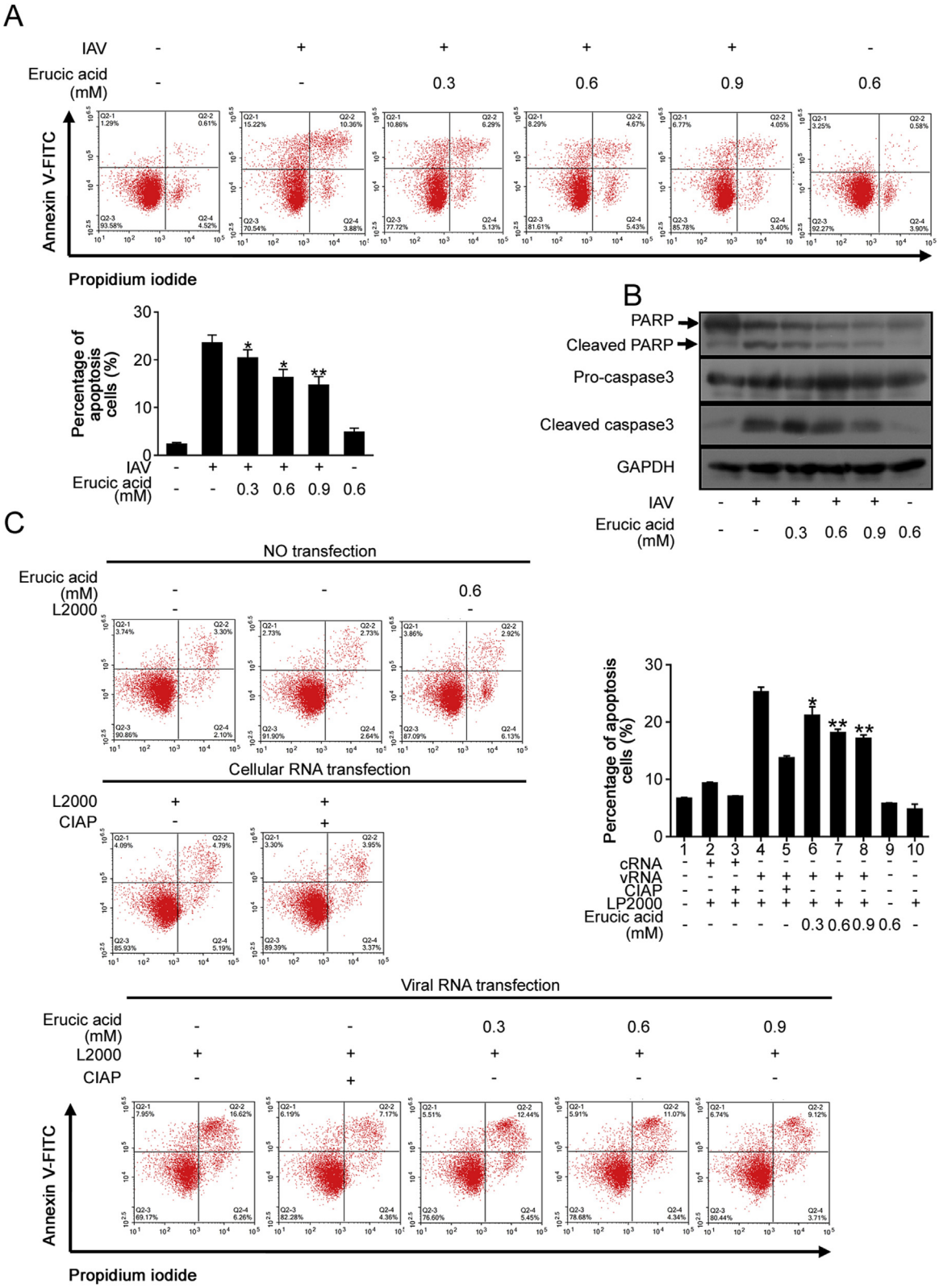

Fig. 5. Erucic acid inhibits IAV-derived vRNA-induced apoptosis and inflammation. IAV-infected cells with erucic acid (0, 0.3, 0.6 and 0.9 mM) treatment were evaluated. (A) Flow cytometry analysis of apoptotic cells using annexin V/PI staining. Data are presented as the mean ± standard error of the mean, representative of three independent experiments. *$P < 0.05$, **$P < 0.01$ vs. IAV-infected. (B) Cleaved caspase-3 and PARP assessed by immunoblotting. vRNA- or cRNA-transfected cells with erucic acid (0, 0.3, 0.6 and 0.9 mM) treatment for 24 h were assessed. (C) Apoptosis analyzed by flow cytometry using annexin V/PI staining. Data are presented as the mean ± standard error of the mean, representative of three independent experiments. *$P < 0.05$, **$P < 0.01$ vs. vRNA-transfected (column 4). (D) Lysates were isolated and used in immunoblotting detection cleaved caspase-3 and PARP. (E) Immunoblotting and (F) Luminex assays were performed to determine the levels of signaling pathways, cytokines and chemokines. Data are presented as the mean ± standard error of the mean, representative of three independent experiments. *$P < 0.05$, **$P < 0.01$, ***$P < 0.001$ vs. vRNA-transfected (column 4). (G) Expression of COX-2 detected by immunoblotting. (H) ELISA assays detecting PGE2 levels. Data are presented as the mean ± standard error of the mean, representative of three independent experiments. ***$P < 0.001$ vs. vRNA-transfected (column 4).

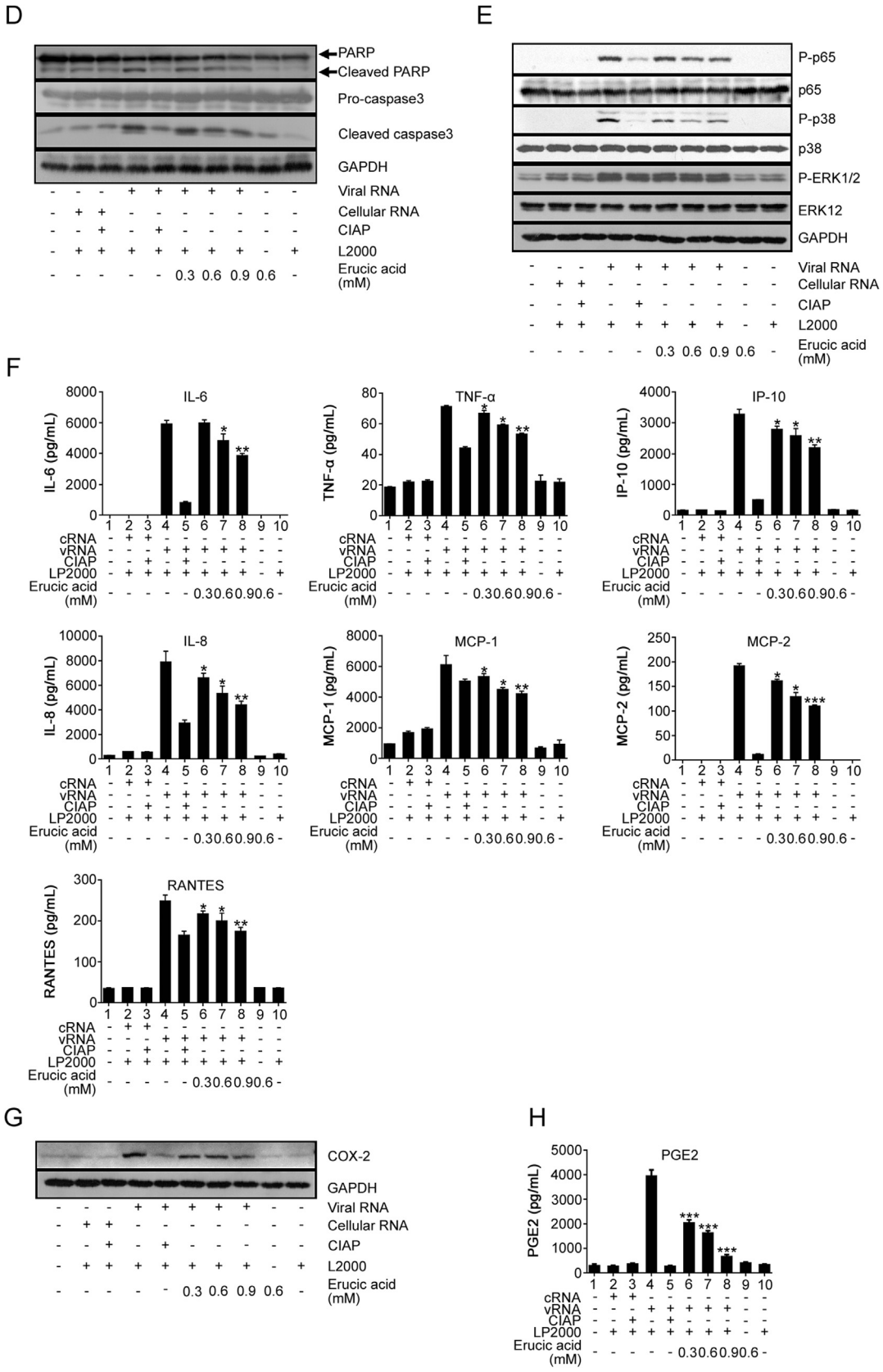

Fig. 5. (*continued*).

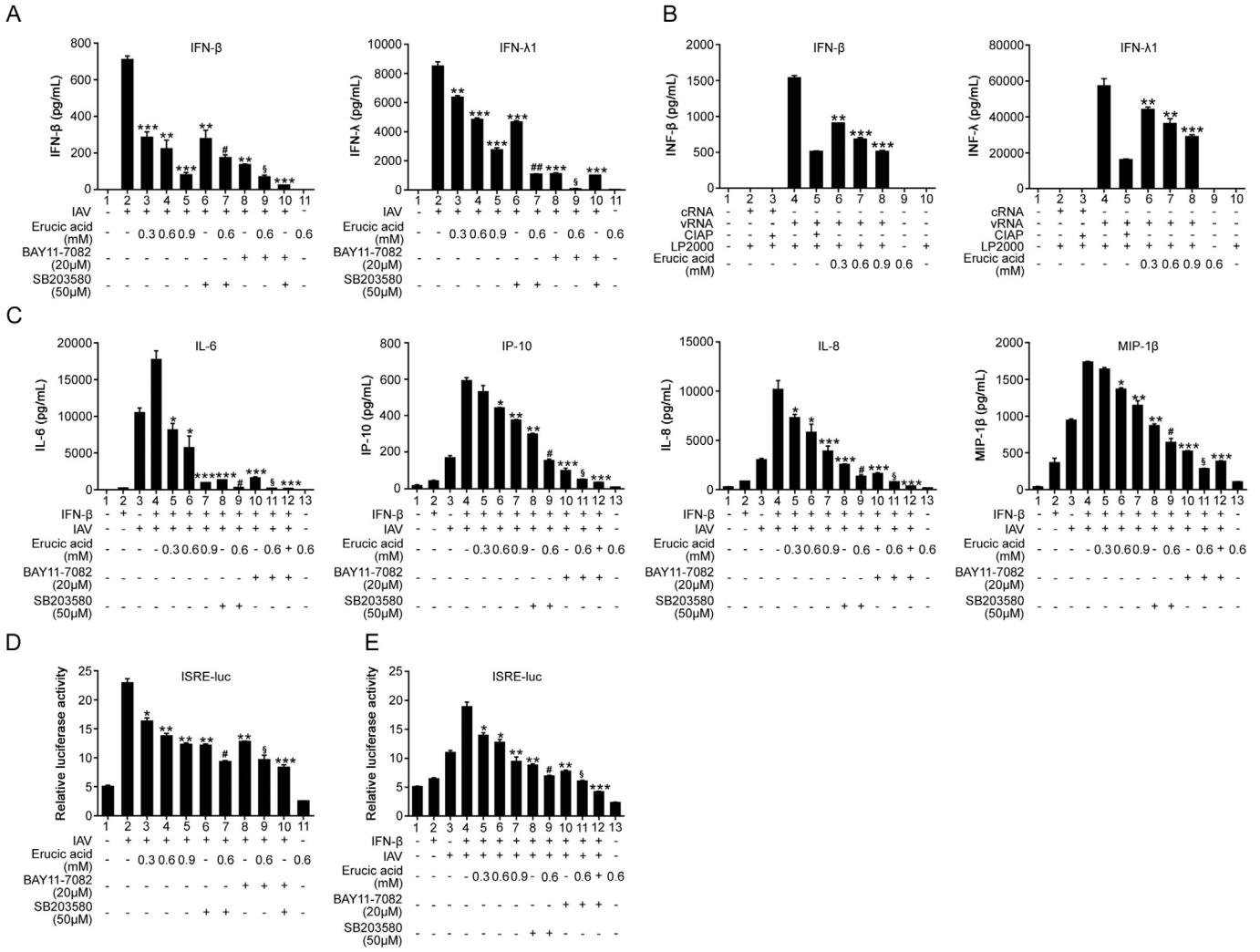

Fig. 6. Erucic acid abrogates IFN-β-amplified pro-inflammatory response in IAV infected cells. (A) Levels of IFN-β and IFN-λ1 were determined by Luminex assays in the culture supernatant of A/PR8/34(H1N1) (MOI = 0.1)-infected A549 cells treated with or without erucic acid. Data are presented the mean ± standard error of the mean, representative of three independent experiments. $^{**}P < 0.01$ and $^{***}P < 0.001$ vs. IAV-infected (column 2); $^{\#}P < 0.05$, $^{\#\#}P < 0.01$ vs. SB203580-treated (column 6); $^{\S}P < 0.05$ vs. BAY11-7082-treated (column 8). (B) Levels of IFN-β and IFN-λ1 were determined by Luminex assays in the culture supernatant of vRNA-transfected cells treated with or without erucic acid. Data are presented as the mean ± standard error of the mean, representative of three independent experiments. $^{**}P < 0.01$ and $^{***}P < 0.001$ vs. vRNA-transfected (column 4). (C) Luminex analysis of pro-inflammatory cytokines secreted in IFN-pre-treated cells prior to influenza A/PR8/34(H1N1) (MOI = 0.1) infection. A549 cells were pre-treated with IFN-β (500 ng/mL) for 4 h, infected with influenza A/PR8/34(H1N1) and treated with or without erucic acid. Data are presented as the mean ± standard error of the mean, representative of three independent experiments. $^{*}P < 0.05$, $^{**}P < 0.01$ and $^{***}P < 0.001$ vs. IFN-pretreated (column 4); $^{\#}P < 0.05$ vs. SB203580-treated (column 8); $^{\S}P < 0.05$ vs. BAY11-7082-treated (column 10). (D) A549 cells were co-transfected with ISRE luciferase reporter plasmid and pRL-TK plasmid. At 6 h post-transfection, cells were infected with A/PR8/34(H1N1) (MOI = 0.1) and treated with or without erucic acid for 24 h; then cells were lysed for luciferase assays. Data are presented as the mean ± standard error of the mean, representative of three independent experiments. $^{*}P < 0.05$, $^{**}P < 0.01$, $^{***}P < 0.001$ vs. IAV-infected (column 2); $^{\#}P < 0.05$ vs. SB203580-treated (column 6); $^{\S}P < 0.05$ vs. BAY11-7082-treated (column 8). (E) A549 cells co-transfected with ISRE luciferase reporter plasmid and pRL-TK plasmid were stimulated with IFN-β (500 ng/mL) for 4 h, infected with A/PR8/34(H1N1) (MOI = 0.1) and treated with or without erucic acid for 24; then cells were harvested for luciferase assays. Luciferase activities were normalized to *Renilla*. Data are presented as the mean ± standard error of the mean, representative of three independent experiments. $^{*}P < 0.05$, $^{**}P < 0.01$ and $^{***}P < 0.001$ vs. IFN-pretreated group (column 4); $^{\#}P < 0.05$ vs. SB203580-treated (column 8); $^{\S}P < 0.05$ vs. BAY11-7082-treated (column 10).

of the NF-κB and p38 MAPK signaling pathways by erucic acid resulted in decreased transcriptional activities of the viral polymerase complex, thereby inhibiting viral replication. Based on these observations, it is probable that the anti-viral property of erucic acid was a result of reducing transcriptional activities of the viral polymerase complex via inhibition of NF-κB and p38 kinase signaling.

Influenza progresses from an initial acute lung injury (ALI) or continues progress to form severe acute respiratory distress syndrome (ARDS), which has been ascribed to the disordered inflammatory processes. Plasma levels of IL-6 are closely correlated with symptoms and fever in human influenza infection [9,46]. Elevation of IL-17 and IP-10 was reported to mediate ALI during the 2009 pandemic influenza A (H1N1) virus infection [47,48]. Development of ALI or ARDS results from the disruption of normal functions of epithelial sodium channels and tight junctions of epithelial-endothelial barriers based on an array of cytokines, including IL-1β, TNF-α, IFN-γ and IL-13 [49–52]. Data obtained in the present study from in vivo and in vitro experiments suggested that pro-inflammatory mediators, including IL-6, TNF-α, MCP-1, IP-10, IL-17 and RANTES, evoked by viral infection or viral product stimulation, were reversed by erucic acid treatment (Figs. 4A, Fig. 5F and Fig. 8B and C). In addition, it was found that erucic acid treatment prevented IAV-mediated symptoms, including piloerection,

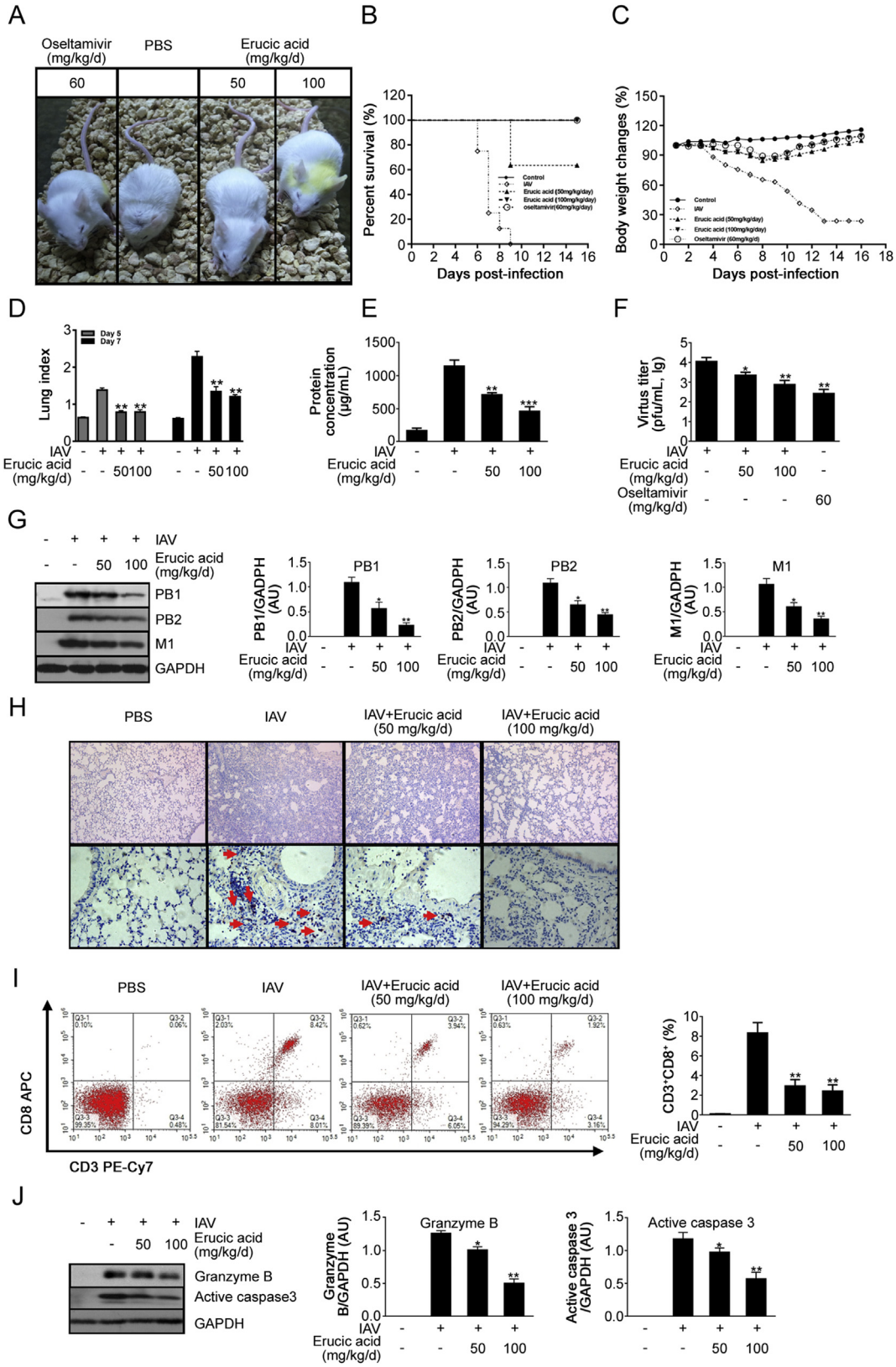

Fig. 7. Erucic acid administration protects against lethal IAV challenge in vivo. Female BALB/c mice received erucic acid (50 and 100 mg/kg/day) for 2 days prior to intranasal inoculation with A/FM1/H1N1 virus (5 LD_{50}). (A) General appearance of mice with or without erucic acid treatment at day 7 p.i. (B–C) Survival rate (B) and weight loss (C) of virus-infected mice with or without erucic acid administration were monitored daily for 14 days ($n = 13–15$/group). Survival curves were compared by log-rank test; $*P < 0.05$, $**P < 0.01$ vs. IAV-infected mice. (D) Lung index (lung/body weight ratios) were measured at day 5 and 7 p.i. Data are presented as the mean ± standard error of the mean. $**P < 0.01$ vs. IAV-infected. (E) Total protein concentration determined by BCA assay in BALF at day 7 p.i. Data are presented as the mean ± standard error of the mean. $**P < 0.01$, $***P < 0.001$ vs. IAV-infected. (F–G) On day 7 p.i., viral titers in lungs were determined by plaque assay and lung homogenate was analyzed for viral proteins (PB1, PB2 and M1) by immunoblotting; GAPDH was used as loading control. Data are presented as the mean ± standard error of the mean. $*P < 0.05$, $**P < 0.01$ vs. IAV-infected. (H) Lung sections were stained with

reduced physical activity, hunched posture, swaying gait and labored breathing, lung injury, including lung index and protein concentration in BALF, and mortality in mice (Figs. 7 A-E). Therefore, it was suggested that protective effects of erucic acid against IAV-mediated morbidity were associated with immunomodulatory properties. Previous studies revealed that activation of NF-κB and p38 kinase signaling is involved in influenza virus-induced dysregulation of pro-inflammatory mediator production. NF-κB deficiency markedly reduces H5N1-mediated hypercytokinemia [17]. Likewise, pharmacological inhibition of NF-κB activation leads to suppressed expression of various cytokines [16,33]. There is no difference in the pattern of NF-κB activation in human primary macrophages with H5N1 and H1N1 virus infection; however, increased p38 activation mediated by H5N1 was observed [53]. p38 kinase inhibition resulted in the reduction of H5N1-mediated cytokine and chemokine levels, such as TNF-α, IFN-β, IFN- λ1 and MCP-1 [21,53].

Furthermore, NF-κB and p38 kinase were reported to regulate the expression of COX-2 [36,37]. Overexpression of COX-2 is implicated in the pathogenesis of avian influenza H5N1 infections [54]. Expression of COX-2 is induced upon viral PAMPs stimulation [55,56]. Consistently, levels of COX-2 and PEG2 were increased in the viral-infected or vRNA (5′ppp-RNA)-stimulated cells, and further reversed by erucic acid treatment (Figs. 4B and C and Fig. 5G and H). Genetic deficiency or pharmacological inhibition of COX-2 significantly decreases virus-mediated inflammation and body temperature changes [57,58]. A study confirmed that the delayed combination treatment of antiviral agents with COX-2 inhibitors protects mice from lethal H5N1 infections [12]. Induction of COX-2-derived PGE2 following IAV infection is not limited to suppressing antiviral innate immune responses and adapts immunity, including macrophage antigen presentation and T cell-mediated immunity [59]. Together with findings that erucic acid inhibited the NF-κB and p38 kinase signaling pathways, it is suggested that erucic acid exerted anti-inflammatory effects via inhibition of NF-κB and p38 kinase signaling during influenza virus infection.

Erucic acid treatment was also found to decrease the expression levels of IFNs in IAV- or vRNA -stimulated cells and BALF form IAV-infected mice lungs (Figs. 6A and B and 8D). IFNs were firmly established as crucial components of innate immunity against viral infection. Type I and III IFNs with their receptor-triggered activation of tripartite transcriptional complex ISGF3, drive expression of antiviral effectors through binding to an ISRE DNA element [60]. IFN-β deficient samples exhibit increased susceptibility to various types of viral infection, including vaccinia virus [61], coxsackievirus B3 [62], Friend retrovirus [63] and influenza virus [64]. However, given immunomodulatory properties of IFNs, the emerging concept is that IFN-β acts in a disease-promoting role in response to viral pathogens. Recent evidence suggests that IAV-mediated IFN-β expression in macrophages increases expression levels of the pro-apoptotic factor TRAIL and contributes to lung injury [38]. It was reported that IFN signaling deficiency attenuates inflammation and protects mice from IAV- or respiratory syncytial virus (RSV)-mediated morbidity [44,65]. In line with this, the current study demonstrated that cells with IFN-β pre-treatment amplified IAV-mediated expression of cytokines that was reversed by erucic acid intervention (Fig. 6C). Further investigations revealed that the underlying mechanism responsible for the amplification of IAV-mediated pro-inflammatory mediator production was associated with the enhancement of the transcriptional activity of the ISGF3 complex induced by IFN-β pre-treatment, while erucic acid treatment reduced the transcriptional activity (Figs. 6D and E). As erucic acid possesses NF-κB and p38 kinase inhibitory activities, the results presented in the current study hypothesized that optimal pro-inflammatory mediator secretion driven by the ISGF3 complex may be associated with NF-κB and p38 kinase activities. These claims were directly confirmed by observations that treatment with NF-κB or p38 kinase inhibitors individually suppressed the transcriptional activity of the ISGF3 complex and amplified pro-inflammatory response elicited by IFN-β pre-treatment. Combination treatment enhanced observed inhibitory effects. Previously, a synergy between the NF-κB and IFN signaling pathways for optimal cytokine IL-12p70 production was described for dendritic cells following LPS or poly (I:C) stimulation [66]. Moreover, inhibition of p38 kinase has been suggested to interfere with IFN signaling transduction by impairing ISGF3 complex formation and STAT1 phosphorylation at serine^{727} [23,67]. Our data added to the aforementioned studies that involvement of NF-κB or p38 kinase signaling may contribute to the IFN-mediated amplification of a detrimental pro-inflammatory response to influenza virus infection.

In vitro data suggested that an increasing percentage of apoptotic cells following influenza virus infection and vRNA stimulation was decreased upon erucic acid treatment (Figs. 5A–D). Similarly, erucic acid reduced levels of pro-apoptotic protease granzyme B as well as apoptosis marker active caspase-3 in vivo (Fig. 7J). During viral infection, apoptosis of the virus-infected cells was regarded as the host defense mechanism to eliminate invading pathogens. However, an increasing evidence suggests that influenza progression has a direct link to the apoptosis of viral-infected cells. Characteristic pathological findings in H5N1- or pandemic H1N1-infected patients with ARDS exhibited severe lung damage involving apoptosis of alveolar epithelial and endothelial cells [68,69]. It has been demonstrated that pro-apoptotic factor TRAIL that is released from recruited macrophages into the atmosphere is significantly associated with the rapid development of IAV-mediated acute lung injury and progression to ARDS [38]. Additionally, CTLs utilize pro-apoptotic factors, including TRAIL, perforin or granzyme B, to trigger apoptosis in IAV-infected cells [70,71], which is as an important limitation of viral replication. However, excessive $CD8^+$ T lymphocytes recruitment contributes to immunopathology in the course of a viral infection. Peripheral blood $CD8^+$ T lymphocytes are more abundant in patients with severe pneumonia than moderate pneumonia [72]. Histological findings of the lungs of novel swine H1N1-infected patients supported that increased $CD8^+$ T lymphocyte and granzyme B^+ expression correlates with diffuse alveolar damage and fatal outcome [73]. Recipient HA-transgenic mice with HA-specific $CD8^+$ cytotoxic T lymphocyte transfer develop progressive lethal lung injury [74]. IAV-specific $CD8^+$ T lymphocytes trigger non-specific apoptosis of bystander alveolar epithelial cells [75]. The current data showed that erucic acid reduced CTL recruitment and cytotoxic granzyme B expression in lungs, which is potentially associated with reduction of IAV-mediated lung injury and mortality.

In conclusion, it was revealed that erucic acid treatment of influenza virus-infected cells resulted in the significant suppression of viral propagation and pro-inflammatory mediator production via

hematoxylin and eosin (scale bar, 200 μm) for histopathological examination and a monoclonal antibody against CD3 (scale bar, 50 μm). (I) Representative flow cytometric plots of $CD3^+CD8^+$ T cells in the BALF at day 7 p.i. Data are presented as the mean ± standard error of the mean ($n = 4$–6). $^{**}P < 0.01$ vs. IAV-infected. (J) Immunoblotting analysis of granzyme B and active caspase-3 in lung homogenates; GAPDH was used as loading control. Data are presented as the mean ± standard error of the mean (n = 3–5). $^{*}P < 0.05$, $^{**}P < 0.01$ vs. IAV-infected.

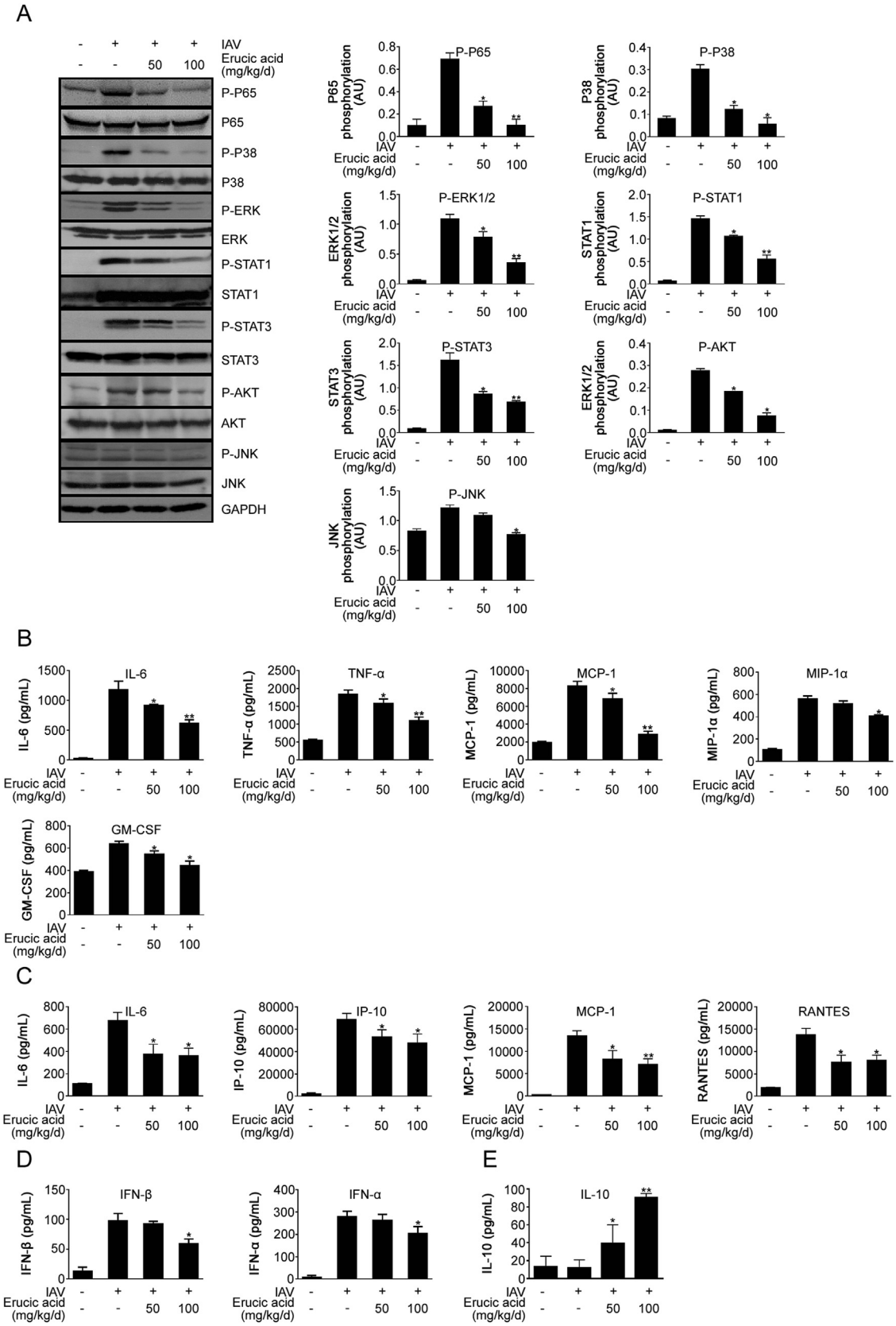

Fig. 8. Erucic acid attenuates excessive pulmonary inflammation upon IAV challenge in vivo. (A) On day 5 p.i., lungs were harvested and homogenized for immunoblot analysis using indicated antibodies. Quantification and normalization of phosphorylated proteins to the internal control GAPDH (right panel). (B–C) Cytokine profiling in BALF (B) and lung homogenates (C) assayed by multiplex analysis. (D) Levels of IFN-α and IFN-β in BALF assayed by Luminex analysis. (E) Levels of IL-10 in lung homogenates assayed by Luminex analysis. Date are presented as the mean ± standard error of the mean. $^{*}P < 0.05$, $^{**}P < 0.01$ vs. IAV-infected.

NF-κB and p38 MAPK signaling inactivation. This further involved interference with ISRE transcriptional activities accompanied by abrogation of the amplification of pro-inflammatory cytokine production in IFN-β pre-treated cells. Moreover, erucic acid protected mice from influenza virus-induced lung injury and improved mortality by attenuating viral load, CTL recruitment and excessive pro-inflammatory mediators. Therefore, it is suggested that erucic acid exerted inhibitory effects on viral replication and modulated virus-evoked excess pro-inflammatory responses that may have potential in the treatment of influenza illness.

Conflicts of interest

The authors declare that there are no conflicts of interest.

Acknowledgments

This study was funded by the National Natural Science Foundation of China (Grant no. 81873065), the Secondary Development Projects of Guangdong Famous and Excellent Traditional Chinese Patent Medicines (Grant no. 20174005), the Natural Science Foundation of Guangdong Province (Grant no. 2018A030310172), and the China Postdoctoral Science Foundation (Grant no. 2017M622652, 2019M652987).

Appendix A. Supplementary data

Supplementary data to this article can be found online at https://doi.org/10.1016/j.jpha.2019.09.005.

References

[1] N.P. Johnson, J. Mueller, Updating the accounts: global mortality of the 1918-1920 "Spanish" influenza pandemic, Bull. Hist. Med. 76 (2002) 105–115.
[2] H.N. Gao, H.Z. Lu, B. Cao, et al., Clinical findings in 111 cases of influenza A (H7N9) virus infection, N. Engl. J. Med. 368 (2013) 2277–2285.
[3] K.K.W. To, K.H.L. Ng, T.-L. Que, et al., Avian influenza A H5N1 virus: a continuous threat to humans, Emerg. Microb. Infect. 1 (2012) e25.
[4] J.-R. Bian, Clinical aspects and cytokine response in adults with seasonal influenza infection, Int. J. Clin. Exp. Med. 7 (2014) 5593–5602.
[5] D. Zamarin, A. Garcia-Sastre, X. Xiao, et al., Influenza virus PB1-F2 protein induces cell death through mitochondrial ANT3 and VDAC1, PLoS Pathog. 1 (2005) e4.
[6] A. Forero, J. Tisoncik-Go, T. Watanabe, et al., The 1918 influenza virus PB2 protein enhances virulence through the disruption of inflammatory and wnt-mediated signaling in mice, J. Virol. 90 (2015) 2240–2253.
[7] A. Kumar, Early versus late oseltamivir treatment in severely ill patients with 2009 pandemic influenza A (H1N1): speed is life, J. Antimicrob. Chemother. 66 (2011) 959–963.
[8] N. Svitek, P.A. Rudd, K. Obojes, et al., Severe seasonal influenza in ferrets correlates with reduced interferon and increased IL-6 induction, Virology 376 (2008) 53–59.
[9] D. Gentile, W. Doyle, T. Whiteside, et al., Increased interleukin-6 levels in nasal lavage samples following experimental influenza A virus infection, Clin. Diagn. Lab. Immunol. 5 (1998) 604–608.
[10] M.D. De Jong, C.P. Simmons, T.T. Thanh, et al., Fatal outcome of human influenza A (H5N1) is associated with high viral load and hypercytokinemia, Nat. Med. 12 (2006) 1203–1207.
[11] R. Salomon, E. Hoffmann, R.G. Webster, Inhibition of the cytokine response does not protect against lethal H5N1 influenza infection, Proc. Natl. Acad. Sci. U.S.A. 104 (2007) 12479–12481.
[12] B.J. Zheng, K.W. Chan, Y.P. Lin, et al., Delayed antiviral plus immunomodulator treatment still reduces mortality in mice infected by high inoculum of influenza A/H5N1 virus, Proc. Natl. Acad. Sci. U.S.A. 105 (2008) 8091–8096.
[13] G. Sharma, D. Champalal Sharma, L. Hwei Fen, et al., Reduction of influenza virus-induced lung inflammation and mortality in animals treated with a phosophodisestrase-4 inhibitor and a selective serotonin reuptake inhibitor, Emerg. Microbes Infect. 2 (2013) e54.
[14] F. Nimmerjahn, D. Dudziak, U. Dirmeier, et al., Active NF-kappaB signalling is a prerequisite for influenza virus infection, J. Gen. Virol. 85 (2004) 2347–2356.
[15] N. Kumar, Z.T. Xin, Y. Liang, et al., NF-kappaB signaling differentially regulates influenza virus RNA synthesis, J. Virol. 82 (2008) 9880–9889.
[16] R. Pinto, S. Herold, L. Cakarova, et al., Inhibition of influenza virus-induced NF-kappaB and Raf/MEK/ERK activation can reduce both virus titers and cytokine expression simultaneously in vitro and in vivo, Antivir. Res. 92 (2011) 45–56.
[17] K. Droebner, S.J. Reiling, O. Planz, Role of hypercytokinemia in NF-kappaB p50-deficient mice after H5N1 influenza A virus infection, J. Virol. 82 (2008) 11461–11466.
[18] I. Mazur, W.J. Wurzer, C. Ehrhardt, et al., Acetylsalicylic acid (ASA) blocks influenza virus propagation via its NF-kappaB-inhibiting activity, Cell Microbiol. 9 (2007) 1683–1694.
[19] D. Marchant, G.K. Singhera, S. Utokaparch, et al., Toll-like receptor 4-mediated activation of p38 mitogen-activated protein kinase is a determinant of respiratory virus entry and tropism, J. Virol. 84 (2010) 11359–11373.
[20] L. Nencioni, G. De Chiara, R. Sgarbanti, et al., Bcl-2 expression and p38MAPK activity in cells infected with influenza A virus: impact on virally induced apoptosis and viral replication, J. Biol. Chem. 284 (2009) 16004–16015.
[21] K.P.Y. Hui, S.M.Y. Lee, C.y. Cheung, et al., Induction of proinflammatory cytokines in primary human macrophages by influenza A virus (H5N1) is selectively regulated by IFN regulatory factor 3 and p38 MAPK, J. Immunol. 182 (2009) 1088–1098.
[22] K. Kujime, S. Hashimoto, Y. Gon, et al., p38 mitogen-activated protein kinase and c-jun-NH2-terminal kinase regulate RANTES production by influenza virus-infected human bronchial epithelial cells, J. Immunol. 164 (2000) 3222–3228.
[23] Y. Borgeling, M. Schmolke, D. Viemann, et al., Inhibition of p38 mitogen-activated protein kinase impairs influenza virus-induced primary and secondary host gene responses and protects mice from lethal H5N1 infection, J. Biol. Chem. 289 (2014) 13–27.
[24] N. Lee, C.K. Wong, P.K. Chan, et al., Hypercytokinemia and hyperactivation of phospho-p38 mitogen-activated protein kinase in severe human influenza A virus infection, Clin. Infect. Dis. 45 (2007) 723–731.
[25] Z. Li, J. Zhao, H. Zhou, et al., Cappariloside A shows antiviral and better anti-inflammatory effects against influenza virus via regulating host IFN signaling, in vitro and vivo, Life Sci. 200 (2018) 115–125.
[26] Z. Luo, L.F. Liu, X.H. Wang, et al., Epigoitrin, an alkaloid from *Isatis indigotica*, reduces H1N1 infection in stress-induced susceptible model in vivo and in vitro, Front. Pharmacol. 10 (2019) 78.
[27] Z. Li, L. Li, H. Zhou, et al., Radix isatidis polysaccharides inhibit influenza a virus and influenza A virus-induced inflammation via suppression of host TLR3 signaling in vitro, Molecules 22 (2017).
[28] Z. Yang, Y. Wang, Z. Zheng, et al., Antiviral activity of *Isatis indigotica root*-derived clemastanin B against human and avian influenza A and B viruses in vitro, Int. J. Mol. Med. 31 (2013) 867–873.
[29] J. Li, B. Zhou, C. Li, et al., Lariciresinol-4-O-beta-D-glucopyranoside from the root of *Isatis indigotica* inhibits influenza A virus-induced pro-inflammatory response, J. Ethnopharmacol. 174 (2015) 379–386.
[30] B. Zhou, J. Li, X. Liang, et al., Transcriptome profiling of influenza A virus-infected lung epithelial (A549) cells with lariciresinol-4-beta-D-glucopyranoside treatment, PLoS One 12 (2017), e0173058.
[31] E. Kim, H.J. Ko, S.J. Jeon, et al., The memory-enhancing effect of erucic acid on scopolamine-induced cognitive impairment in mice, Pharmacol. Biochem. Behav. 142 (2016) 85–90.
[32] L.J. Reed, H. Muench, A simple method of estimating fifty percent endpoints, Am. J. Epidemiol. 27 (1938) 493–497.
[33] B. Zhou, Z. Yang, Q. Feng, et al., Aurantiamide acetate from *Baphicacanthus cusia root* exhibits anti-inflammatory and anti-viral effects via inhibition of the NF-kappaB signaling pathway in influenza A virus-infected cells, J. Ethnopharmacol. (2017).
[34] S. Ludwig, Targeting cell signalling pathways to fight the flu: towards a paradigm change in anti-influenza therapy, J. Antimicrob. Chemother. 64 (2009) 1–4.
[35] I. Ramos, A. Fernandez-Sesma, Modulating the innate immune response to influenza A virus: potential therapeutic use of anti-inflammatory drugs, Front. Immunol. 6 (2015).
[36] P.D. N'Guessan, S. Hippenstiel, M.O. Etouem, et al., Streptococcus pneumoniae induced p38 MAPK- and NF-kappaB-dependent COX-2 expression in human lung epithelium, Am. J. Physiol. Lung Cell Mol. Physiol. 290 (2006) L1131–1138.
[37] C.A. Singer, K.J. Baker, A. McCaffrey, et al., p38 MAPK and NF-kappaB mediate COX-2 expression in human airway myocytes, Am. J. Physiol. Lung Cell Mol. Physiol. 285 (2003) L1087–1098.
[38] K. Högner, T. Wolff, S. Pleschka, et al., Macrophage-expressed IFN-β contributes to apoptotic alveolar epithelial cell injury in severe influenza virus pneumonia, PLoS Pathog. 9 (2013), e1003188.
[39] R. Besch, H. Poeck, T. Hohenauer, et al., Proapoptotic signaling induced by RIG-I and MDA-5 results in type I interferon-independent apoptosis in human melanoma cells, J. Clin. Investig. 119 (2009) 2399–2411.
[40] J.S. Rossman, R.A. Lamb, Autophagy, apoptosis, and the influenza virus M2 protein, Cell Host Microbe 6 (2009) 299–300.
[41] C. Zhang, Y. Yang, X. Zhou, et al., The NS1 protein of influenza A virus interacts with heat shock protein Hsp90 in human alveolar basal epithelial cells: implication for virus-induced apoptosis, Virol. J. 8 (2011) 181.
[42] D. Panne, T. Maniatis, S.C. Harrison, An atomic model of the interferon-beta enhanceosome, Cell 129 (2007) 1111–1123.
[43] K. Onoguchi, M. Yoneyama, A. Takemura, et al., Viral infections activate types I and III interferon genes through a common mechanism, J. Biol. Chem. 282 (2007) 7576–7581.
[44] S. Davidson, S. Crotta, T.M. McCabe, et al., Pathogenic potential of interferon αβ in acute influenza infection, Nat. Commun. 5 (2014) 3864.

[45] Y. Chi, Y. Zhu, T. Wen, et al., Cytokine and chemokine levels in patients infected with the novel avian influenza A (H7N9) virus in China, J. Infect. Dis. 208 (2013) 1962–1967.
[46] L. Kaiser, R.S. Fritz, S.E. Straus, et al., Symptom pathogenesis during acute influenza: interleukin-6 and other cytokine responses, J. Med. Virol. 64 (2001) 262–268.
[47] W. Wang, P. Yang, Y. Zhong, et al., Monoclonal antibody against CXCL-10/IP-10 ameliorates influenza A (H1N1) virus induced acute lung injury, Cell Res. 23 (2013) 577–580.
[48] C. Li, P. Yang, Y. Sun, et al., IL-17 response mediates acute lung injury induced by the 2009 pandemic influenza A (H1N1) virus, Cell Res. 22 (2012) 528–538.
[49] J.M. Mullin, K.V. Snock, Effect of tumor necrosis factor on epithelial tight junctions and transepithelial permeability, Cancer Res. 50 (1990) 2172–2176.
[50] J. Roux, H. Kawakatsu, B. Gartland, et al., Interleukin-1β decreases expression of the epithelial sodium channel alpha-subunit in alveolar epithelial cells via a p38 MAPK-dependent signaling pathway, J. Biol. Chem. 280 (2005) 18579–18589.
[51] L.J. Galietta, P. Pagesy, C. Folli, et al., IL-4 is a potent modulator of ion transport in the human bronchial epithelium in vitro, J. Immunol. 168 (2002) 839–845.
[52] L.J. Galietta, C. Folli, C. Marchetti, et al., Modification of transepithelial ion transport in human cultured bronchial epithelial cells by interferon-γ, Am. J. Physiol. Lung Cell Mol. Physiol. 278 (2000) L1186–1194.
[53] D.C. Lee, C.Y. Cheung, A.H. Law, et al., p38 mitogen-activated protein kinase-dependent hyperinduction of tumor necrosis factor alpha expression in response to avian influenza virus H5N1, J. Virol. 79 (2005) 10147–10154.
[54] S.M. Lee, C.Y. Cheung, J.M. Nicholls, et al., Hyperinduction of cyclooxygenase-2-mediated proinflammatory cascade: a mechanism for the pathogenesis of avian influenza H5N1 infection, J. Infect. Dis. 198 (2008) 525–535.
[55] N.S. Kirkby, A.K. Zaiss, W.R. Wright, et al., Differential COX-2 induction by viral and bacterial PAMPs: consequences for cytokine and interferon responses and implications for anti-viral COX-2 directed therapies, Biochem. Biophys. Res. Commun. 438 (2013) 249–256.
[56] S.E. Dudek, K. Nitzsche, S. Ludwig, et al., Influenza A viruses suppress cyclooxygenase-2 expression by affecting its mRNA stability, Sci. Rep. 6 (2016) 27275.
[57] M.A. Carey, J.A. Bradbury, J.M. Seubert, et al., Contrasting effects of cyclooxygenase-1 (COX-1) and COX-2 deficiency on the host response to influenza A viral infection, J. Immunol. 175 (2005) 6878–6884.
[58] M.A. Carey, J.A. Bradbury, Y.D. Rebolloso, et al., Pharmacologic inhibition of COX-1 and COX-2 in influenza A viral infection in mice, PLoS One 5 (2010), e11610.
[59] F. Coulombe, J. Jaworska, M. Verway, et al., Targeted prostaglandin E2 inhibition enhances antiviral immunity through induction of type I interferon and apoptosis in macrophages, Immunity 40 (2014) 554–568.
[60] A.J. Sadler, B.R. Williams, Interferon-inducible antiviral effectors, Nat. Rev. Immunol. 8 (2008) 559–568.
[61] R. Deonarain, A. Alcami, M. Alexiou, et al., Impaired antiviral response and alpha/beta interferon induction in mice lacking beta interferon, J. Virol. 74 (2000) 3404–3409.
[62] R. Deonarain, D. Cerullo, K. Fuse, et al., Protective role for interferon-beta in coxsackievirus B3 infection, Circulation 110 (2004) 3540–3543.
[63] N. Gerlach, S. Schimmer, S. Weiss, et al., Effects of type I interferons on Friend retrovirus infection, J. Virol. 80 (2006) 3438–3444.
[64] I. Koerner, G. Kochs, U. Kalinke, et al., Protective role of beta interferon in host defense against influenza A virus, J. Virol. 81 (2007) 2025–2030.
[65] M. Goritzka, L.R. Durant, C. Pereira, et al., Alpha/beta interferon receptor signaling amplifies early proinflammatory cytokine production in the lung during respiratory syncytial virus infection, J. Virol. 88 (2014) 6128–6136.
[66] G. Gautier, M. Humbert, F. Deauvieau, et al., A type I interferon autocrine-paracrine loop is involved in Toll-like receptor-induced interleukin-12p70 secretion by dendritic cells, J. Exp. Med. 201 (2005) 1435–1446.
[67] K.C. Goh, S.J. Haque, B.R. Williams, p38 MAP kinase is required for STAT1 serine phosphorylation and transcriptional activation induced by interferons, EMBO J. 18 (1999) 5601–5608.
[68] V.L. Capelozzi, E.R. Parra, M. Ximenes, et al., Pathological and ultrastructural analysis of surgical lung biopsies in patients with swine-origin influenza type A/H1N1 and acute respiratory failure, Clinics (Sao Paulo) 65 (2010) 1229–1237.
[69] M. Uiprasertkul, R. Kitphati, P. Puthavathana, et al., Apoptosis and pathogenesis of avian influenza A (H5N1) virus in humans, Emerg. Infect. Dis. 13 (2007) 708–712.
[70] E. Ishikawa, M. Nakazawa, M. Yoshinari, et al., Role of tumor necrosis factor-related apoptosis-inducing ligand in immune response to influenza virus infection in mice, J. Virol. 79 (2005) 7658–7663.
[71] J.E. Kohlmeier, T. Cookenham, A.D. Roberts, et al., Type I interferons regulate cytolytic activity of memory CD8(+) T cells in the lung airways during respiratory virus challenge, Immunity 33 (2010) 96–105.
[72] J.E. Kim, S. Bauer, K.S. La, et al., CD4+/CD8+ T lymphocytes imbalance in children with severe 2009 pandemic influenza A (H1N1) pneumonia, Korean J. Pediatr. 54 (2011) 207–211.
[73] T. Mauad, L.A. Hajjar, G.D. Callegari, et al., Lung pathology in fatal novel human influenza A (H1N1) infection, Am. J. Respir. Crit. Care Med. 181 (2010) 72–79.
[74] R.I. Enelow, A.Z. Mohammed, M.H. Stoler, et al., Structural and functional consequences of alveolar cell recognition by CD8(+) T lymphocytes in experimental lung disease, J. Clin. Investig. 102 (1998) 1653–1661.
[75] C.E. van de Sandt, M. Barcena, A.J. Koster, et al., Human CD8(+) T cells damage noninfected epithelial cells during influenza virus infection in vitro, Am. J. Respir. Cell Mol. Biol. 57 (2017) 536–546.